

RESEARCH ARTICLE

Development and dynamics of a novel couple-constrained parallel wrist with three measuring force flexible fingers

Yang Lu^{1,2}, Zefeng Chang¹ and Yi Lu¹ 

¹College of Mechanical Engineering, Yanshan University, Qinhuangdao, Hebei, 066004, PR China and ²Harbin Electric Corporation (Qinhuangdao) Heavy Equipment Company Limited, Qinhuangdao, Hebei, 066004, PR China

Corresponding authors: Yi Lu, Yang Lu; Emails: luyi@ysu.edu.cn, deersheepxn@163.com

Received: 12 March 2023; **Revised:** 7 April 2023; **Accepted:** 19 April 2023; **First published online:** 16 June 2023

Keywords: kinematics; dynamics; parallel manipulator; Jacobian matrix; Hessian matrix; couple-constraint

Abstract

A novel couple-constrained parallel wrist with three measuring force flexible fingers is designed for grabbing heavy objects and measuring grabbed forces. Its prototype is developed, its dynamics model is established, and its grabbing forces are measured. First, using the extended formulas of the skew-symmetric matrix, the kinematic formulas are derived for solving the Jacobian/Hessian matrices and the general velocity/acceleration of the moving links in the couple-constrained parallel wrist. Second, a dynamics model is established for solving the dynamic actuation forces, the couple-constrained forces, and the torque in the couple-constrained parallel wrist. Third, the theoretical solutions of the kinematics/dynamics of the couple-constrained parallel wrist are verified using a simulation mechanism. Finally, the grabbing forces of the three flexible fingers are measured and analyzed.

Nomenclature

| | |
|---------------------------|--|
| R, P | revolute, prismatic joints |
| U, S | universal, spherical joints |
| DOF | degree of freedom |
| m_p, B | moving platform and base of parallel wrist |
| o, O | original points of m_p, B |
| $\{m\}$ | coordinate system $o-xyz$ of m_p at o , |
| $\{B\}$ | coordinate system $O-XYZ$ of B at O , |
| $s(\xi)$ | skew-symmetric matrix of vector ξ |
| $\{i_j\}$ | coordinate system attached on the j th finger |
| w_j, y_j' | tip point, input velocity of the j th finger |
| V_{wj} | output velocity of the j th finger at w_j in $\{B\}$ |
| J_{wj} | Jacobian matrix of the j th finger |
| iR_j | rotational matrix from $\{i_j\}$ to $\{B\}$ |
| V_{pr} | general input velocity of parallel wrist |
| A_{pr} | general input acceleration of parallel wrist |
| V_r | general input velocity of parallel wrist, finger |
| A_r | input acceleration of parallel wrist, finger |
| V_f | general input velocity of fingers |
| J, H | Jacobian, Hessian matrix of parallel wrist |
| g_i | moving link in $r_i(g=p, q, i=0, 1, 2, 3)$ |
| ω_i, ε_i | angular velocity acceleration of r_i |

| | |
|--------------------------------------|---|
| $\mathbf{v}_{g_i}, \mathbf{a}_{g_i}$ | translational velocity acceleration of g_i in r_i |
| $\mathbf{V}_{g_i}, \mathbf{A}_{g_i}$ | general (velocity, acceleration) of g_i in r_i |
| $\mathbf{J}_{v_{g_i}}$ | translational Jacobian matrices of g_i in r_i |
| $\mathbf{J}_{\omega_{g_i}}$ | rotational Jacobian matrices of g_i in r_i |
| $\mathbf{H}_{v_{g_i}}$ | translational Hessian matrices of g_i in r_i |
| $\mathbf{H}_{\omega_{g_i}}$ | rotational Hessian matrices of g_i in r_i |
| $\mathbf{J}_{g_i}, \mathbf{H}_{g_i}$ | general Jacobian, Hessian matrix of g_i in r_i |

1. Introduction

It has been an interesting and challenging issue in the robot industry to design and develop various industrial grippers and the finger mechanisms [1–4] to grab heavy objects and to measure grabbing forces. Comparing with the serial mechanism, a parallel mechanism has several advantages, such as the high rigidity, short kinematic chain, high kinematic precision, and large capability of load bearing [5, 6]. Therefore, parallel mechanisms have been applied in the parallel machine tools, worktables, and parallel legs [7, 8], and some three degrees of freedom (DOF) parallel mechanisms are synthesized [5, 6, 9]. Currently, some significant advances have been made in sophisticated biomimetic robotics systems using parallel mechanisms and several dexterous multifingers [3, 4, 10]. In this aspect, Spencer et al. presented the design and experimental results for a 16-finger highly underactuated microspine gripper for application in the deep ocean [11]. Jin et al. designed a dexterous hand based on several parallel finger structures [12]. Fang et al. synthesized some parallel dexterous hands with a parallel finger structure based on Lie group [13]. He et al. designed a finger mechanism with a redundant serial-parallel hybrid topology [14]. Zheng et al. proposed a 12-section cable-driven hyper redundant manipulator with a puller follower controller [15]. Li et al. developed a two-finger dexterous bionic hand with six DOFs [16]. Isaksson et al. designed a 5-DOF redundant platform in order to transform the redundant platform motion into the motion of a grasper [17]. Geng et al. presented a 3-DOF parallel micro-gripper and analyzed its kinematics [18]. However, the existing grippers formed by cable-driven redundant manipulator may have a less capability for grabbing the heavy object since a cable-driven finger has a lower load bearing capability.

The gripper formed by the links, gears, and cams may have both quite complex structure and large volume. In other hand, some existing 3-DOF parallel mechanisms may include some structure decoupling constraints which are sensitive to the manufacturing errors, so that their kinematic precision may be decreased and their manufacturing becomes difficult [19]. The workspace of some existing 3-DOF parallel mechanisms may be small, so that the dexterity of the gripper formed by them is reduced. Hence, it has been a significant issue to develop a gripper using a 3-DOF parallel mechanism which is not sensitive to the manufacturing errors and has a high rigidity and a large workspace in order to grab heavy objects in large workspace and to measure grabbing force.

The main motivation of this paper is to develop a novel couple-constrained parallel wrist with three measuring force flexible fingers in order to increase the rigidity, the kinematic precision, and the capability of grabbing heavy object, and to measure grabbing load and to reduce impact grabbing force when the finger contacts with an object. The developed couple-constrained parallel wrist with three measuring force flexible fingers has the following merits:

1. Its parallel wrist contains a planar couple-constrained actuation mechanism P_a and a SP (spherical joint-prismatic joint) center passive constrained limb r_0 . Its kinematic precision and rigidity are increased by P_a and r_0 . Using r_0 , the structure coupling constraints of the parallel wrist can be transformed into the structure decoupling constraints which are not sensitive to the manufacturing errors [7]. Thus, both the kinematic precision and the rigidity of the parallel wrist can be increased. In addition, the manufacturing of the parallel wrist becomes easy.

2. The number of the links in the parallel wrist is reduced, and both the capability of load-bearing and the workspace are increased by P_a since each of revolute joints in P_a has larger capability of load-bearing and larger rotational angle than that of spherical or universal joint.
3. It can be used to grab heavy objects with various shapes. The contacting force between a fingertip and the grabbed object can be solved by measuring the force of the finger sensor.
4. A large grabbed impact can be reduced greatly by a pre-pressured spring installed in each finger.

However, the kinematics/dynamics models of the developed couple-constrained parallel wrist with three flexible finger have not been established; the grabbed forces have not been measured and the grabbing performances have not been discovered and analyzed yet. For this reason, the kinematics/dynamics and grabbing capability of the developed couple-constrained parallel wrist with three flexible finger are studied in this paper. Several contributions are conducted as follows:

1. Develop a novel prototype of a couple-constrained parallel wrist with three flexible fingers.
2. Derive Jacobian and Hessian matrices of the moving links such as the moving platform, the piston rods, the cylinder rods in four different limbs, and the connection rod in parallel wrist. Establish the kinematics models for solving the general velocity and acceleration of the moving links in order to establish dynamics model.
3. Establish a dynamics model for solving the dynamic actuation forces, the dynamic constrained forces and torque of the developed gripper. Verify the theoretical solutions by its simulation mechanism. Construct a workspace of the couple-constrained parallel wrist with three flexible fingers.

2. Kinematics of couple-constrained parallel wrist with three measuring force flexible finger

2.1 Structure performance analysis of prototype

A prototype of the couple-constrained parallel wrist with three measuring force flexible finger is developed in Yanshan University, see Fig. 1.

The kinematics model of the couple-constrained parallel wrist with the coordinate system and the couple-constrained forces is shown in Fig. 2. Let (S, P, P, R, U) denote (the spherical, actuation prismatic, prismatic, revolute, and universal) joint. The couple-constrained parallel wrist includes a moving platform m_p , a fixed base B , a SPU (spherical joint - actuation prismatic joint - universal joint) actuation limb r_2 with a linear actuator, a SP-type center passive constrained rod r_0 , a planar couple-constrained actuation mechanism P_a , and three flexible fingers installed with sensors and springs. Here, P_a is formed by 2 RPRR (revolute joint - actuation prismatic joint - revolute joint - revolute joint) linear actuation limbs r_i ($i = 1, 3$), a connection rod L and m_p . m_p is a quaternary link with three connection points b_i ($i = 1, 2, 3$) and a central connection point o . L is a ternary link with 2 connection joints at B_i ($i = 1, 3$) and a center connection point B_L . B is a ternary link with two connection points (B_L, B_2) and a central connection point O .

Each of r_i ($i = 1, 3$) has a linear actuator. The lower ends of r_i are connected with the two ends of L at points B_i ($i = 1, 3$) by the revolute joints R_i ($i = 1, 3$). The upper end of r_i is connected with m_p at b_i using the universal joint U_i formed by two crossed revolute joints R_{i1} and R_{i2} . r_0 is formed by a piston rod r_{p0} and a cylinder r_{q0} . r_{p0} is perpendicular to m_p , and the upper end of r_{p0} is fixed onto m_p at o . The lower end of r_{p0} is coaxially connected with r_{q0} by p joint. The lower end of r_{q0} is connected with B at O by S joint. L is connected with B at B_L by a revolute joint R_L . The upper end of r_2 is connected with m_p at b_2 by U joint. The lower end of r_2 is connected with B at B_2 by S joint. b_i ($i = 1, 2, 3$) are uniformly located in the same circumference of m_p . B_i ($i = 1, 3$) and B_2 are located in the same circumference of B . Let $(\parallel, \perp, |)$ be the parallel constraint, perpendicular constraint, and collinear constraint, respectively. Let l_v be a line from b_1 to b_3 . The geometric constraints $\{R_L|L; L|X, R_i \perp L (i = 1, 3); R_1 \parallel R_3 \parallel R_{12} \parallel R_{32}; R_i \perp r_i;$

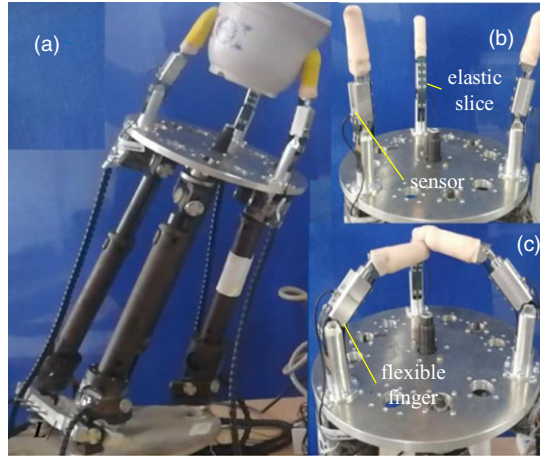


Figure 1. Prototype of couple-constrained parallel wrist with three flexible fingers (a) The open and closed poses of three fingers (b), (c).

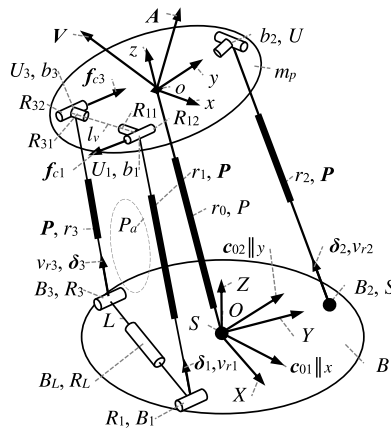


Figure 2. Kinematics model of couple-constrained parallel wrist.

$R_{11} \perp R_{31}; R_{11} \perp R_{12}; R_{31} \perp R_{32}; x \parallel l_v; z \perp m; Z \perp B$ are satisfied. In this case, R_{11} and R_{31} are always kept in the same rotation. Based on a revised Grübler–Kutzbach equation [6], the DOF of the couple-constrained parallel wrist is calculated as follows:

$$\begin{aligned}
 M &= 6(n_0 - n - 1) + \sum M_i + \zeta - M_0 \\
 &= 6 \times (10 - 12 - 1) + 18 + 3 = 3
 \end{aligned}
 \tag{1}$$

The number of the links is $n_0 = 10$ including one m_p with the piston rod of r_0 , one cylinder of r_0 , 1 B , 1 L , 3 cylinders of r_i ($i = 1, 2, 3$), and three piston rods of r_i ; the number of the kinematic pairs is $n = 12$ including $\{R_1, R_3, R_L, U_1, U_3, 2S, 1U, 4P\}$; the sum of local DoFs of the kinematic pairs is $\sum M_i = 18$ since $(R_1, R_3, R_L, 4P)$ provide seven local DOFs, $2S$ provide six local DOFs, $1U$ provide two local DOFs, and $\{U_1, U_3\}$ provide three local DOFs because R_{11} and R_{31} are with the same rotation; the redundant constraint is $\zeta = 3$ for P_a ; and passive DOF is $M_0 = 0$.

DOF of the flexible finger is calculated as 1 in ref. [20].

2.2 Kinematics model of moving platform

The couple-constrained parallel wrist includes several moving links. Let $\{m\}$ be a coordinate system o - xyz fixed on m_p at o , $\{B\}$ be a coordinate system O - XYZ fixed on B at O . Let $\{r_i, \delta_i (i = 1, 2, 3)\}$ be the vector of the actuation limb r_i and its unit vector, respectively, e_i be the vector from o to b_i , $\{^m b_i, b_i (i = 1, 2, 3)\}$ be the vector position of connection point b_i on m_p in $\{m\}$ and $\{B\}$, respectively. Let $\{B_i (i = 1, 2, 3)\}$ be the vector position of the connection point B_i on B in $\{B\}$, (o, X_o, Y_o, Z_o) be the vector position of point o on m_p in $\{B\}$ and its three components. Let $(x_l, x_m, x_n, y_l, y_m, y_n, z_l, z_m, z_n)$ be the nine orientation parameters of m_p in $\{B\}$, (α, β, γ) be three Euler angles. Let $e_i = e (i = 1, 2, 3)$ be the distance from o to b_i , E_i be the distance from O to B_i , φ_i be the angle between x and the line from o to b_i , L be the unit vector of L , l_v be the unit vector of l_v , φ be one of $(\alpha, \beta, \gamma, \varphi_i, \theta_6)$. Set $s_\varphi = \sin\varphi$, $c_\varphi = \cos\varphi$, $t_\varphi = \tan\varphi$. Let ${}^B_m R$ be a rotation matrix from $\{m\}$ to $\{B\}$ in the order of YXZ . $\{{}^B_m R, {}^m b_i, b_i, B_i (i = 1, 2, 3)\}$ are represented as follows:

$${}^B_m R = \begin{pmatrix} x_l = c_\beta & y_l = s_\beta s_\gamma & z_l = s_\beta c_\gamma \\ x_m = s_\alpha c_\beta & y_m = c_\alpha c_\gamma - s_\alpha c_\beta s_\gamma & z_m = -c_\alpha s_\gamma - s_\alpha c_\beta c_\gamma \\ x_n = -c_\alpha s_\beta & y_n = s_\alpha c_\gamma + c_\alpha c_\beta s_\gamma & z_n = -s_\alpha s_\gamma + c_\alpha c_\beta c_\gamma \end{pmatrix} \tag{2a}$$

$${}^m b_i = \begin{pmatrix} X_{bi} \\ Y_{bi} \\ Z_{bi} \end{pmatrix} = e_i \begin{pmatrix} c_{\varphi_i} \\ s_{\varphi_i} \\ 0 \end{pmatrix}, B_i = \begin{pmatrix} X_{Bi} \\ Y_{Bi} \\ Z_{Bi} \end{pmatrix} = E_i \begin{pmatrix} c_{\varphi_i} \\ s_{\varphi_i} \\ 0 \end{pmatrix}, \tag{2b}$$

$$l_v = x = \begin{pmatrix} c_\beta \\ s_\alpha s_\beta \\ -c_\alpha s_\beta \end{pmatrix}, L = X = \begin{pmatrix} 1 \\ 0 \\ 0 \end{pmatrix}, \begin{matrix} \varphi_1 = 330^\circ, \\ \varphi_2 = 90^\circ, \\ \varphi_3 = 210^\circ \end{matrix}$$

$$o = \begin{pmatrix} X_o \\ Y_o \\ Z_o \end{pmatrix}, b_i = {}^B_m R {}^m b_i + o = \begin{pmatrix} e_i c_{\varphi_i} x_l + e_i s_{\varphi_i} y_l + X_o \\ e_i c_{\varphi_i} x_m + e_i s_{\varphi_i} y_m + Y_o \\ e_i c_{\varphi_i} x_n + e_i s_{\varphi_i} y_n + Z_o \end{pmatrix} \tag{2c}$$

The formulas for solving the inverse displacement $r_i (i = 1, 2, 3)$ are derived from Eqs. (2a), (2b), (2c) as follows:

$$(l_v r_i L) = 0 \rightarrow \begin{vmatrix} x_l & x_m & x_n \\ X_{b1} - X_{B1} & Y_{b1} - Y_{B1} & Z_{b1} - Z_{B1} \\ 1 & 0 & 0 \end{vmatrix} = 0$$

$$x_m (Z_{b1} - Z_{B1}) - x_n (Y_{b1} - Y_{B1}) = 0 \rightarrow \tag{3a}$$

$$c_\gamma = \frac{E_1 s_{\varphi_1} c_\alpha - s_\alpha Z_o - c_\alpha Y_o}{e_1 s_{\varphi_1}}$$

$$r_i = b_i - B_i = \begin{pmatrix} e_i c_{\varphi_i} x_l + e_i s_{\varphi_i} y_l + X_o - E_i c_{\varphi_i} \\ e_i c_{\varphi_i} x_m + e_i s_{\varphi_i} y_m + Y_o - E_i s_{\varphi_i} \\ e_i c_{\varphi_i} x_n + e_i s_{\varphi_i} y_n + Z_o \end{pmatrix}, \tag{3b}$$

$$r_0^2 = X_o^2 + Y_o^2 + Z_o^2, \delta_i = \frac{r_i}{|r_i|}, i = 1, 2, 3$$

It is found from the structure performance in Fig. 2 that the parallel wrist includes two independent constrained forces $f_{c0i} (i = 1, 2)$ and two couple-constrained forces $f_{ci} (i = 1, 3)$. $f_{c0i} (i = 1, 2)$ are exerted onto r_0 at O , f_{ci} are exerted onto m_p at $b_i (i = 1, 3)$. Let (f_{c0i}, c_{i0}) be the scalar and unit vectors of f_{c0i} . Since $f_{c0i} (i = 1, 2)$ do not generate any power during the moving of r_0 , $(f_{c0i} \perp r_0, f_{c0i} | O)$ must be satisfied. Since there are $(x \perp r_0, y \perp r_0)$, $(c_{01} = x, c_{02} = y)$ are satisfied. Based on the principle of virtual power, $f_{c0i} (i = 1, 2)$ and their constrained torques satisfy

$$f_{c0i} c_{0i} \cdot v + (f_{c0i} c_{0i} \times o) \cdot \omega = 0 \rightarrow$$

$$(x^T \quad (x \times o)^T) V = 0, (y^T \quad (y \times o)^T) V = 0 \tag{4}$$

here, x, y , and o are the unit vectors of x , the unit vector of y and the vector of o in $\{B\}$, respectively.

Let (f_{ci}, c_i) be the scalar and unit vectors of f_{ci} . Since f_{ci} ($i = 1, 3$) do not generate any power during the moving of m_p , $(c_i \parallel R_{i2}$ and $c_3 = -c_1)$ must be satisfied. Let t_{ci} ($i = 1, 3$) be the constrained torques exerted onto L . Let L be the unit vector of L . $\{(f_{ci} \times r_i) \cdot L = t_{ci}, (i = 1, 3); t_{c1} = t_{c3}, t_{c1} \parallel L\}$ are satisfied based on the balancing condition of the constrained torques. Therefore, there are

$$\begin{aligned}
 & (r_1 \times f_{c1}c_1 + r_3 \times f_{c3}c_3) \cdot L = 0 \rightarrow \tag{5} \\
 & f_{c3} = -\frac{(r_1 \times c_1) \cdot L}{(r_3 \times c_3) \cdot L} f_{c1}, c_1 = x \times \delta_1, c_3 = -c_1
 \end{aligned}$$

Since neither the couple-constrained forces f_{ci} ($i = 1, 3$) nor the couple-constrained torques $e_i \times f_{ci}$ generate power, $(f_{c1} \parallel f_{c3}, c_i \perp \delta_i, c_i \parallel R_i)$ are satisfied. It is known from the principle of virtual power that the couple-constrained wrench must satisfy

$$\begin{aligned}
 & (f_{c1}c_1 + f_{c3}c_3) \cdot v + (e_1 \times f_{c1}c_1 + e_3 \times f_{c3}c_3) \cdot \omega = 0, \tag{6} \\
 & e_3 = e_1 - l_1x
 \end{aligned}$$

Substitute Eq. (5) for Eq. (6), it leads to

$$\begin{aligned}
 & \{(r_3 \times c_3) \cdot L\} c_1 - \{(r_1 \times c_1) \cdot L\} c_3 \cdot v + \{e_1 \times [(r_3 \times c_3) \cdot L] \cdot c_1 \\
 & - [(r_1 \times c_1) \cdot L] \cdot c_3\} + l_1x \times \{(r_1 \times c_1) \cdot L\} \cdot c_3 \cdot \omega = 0 \tag{7}
 \end{aligned}$$

Eq. (7) can be simplified as below:

$$c \cdot v + \tau \cdot \omega = 0, (c^T \quad \tau^T) V = 0 \tag{8}$$

The items c and τ in Eq. (8) are derived from Eq. (7) and $c_3 = -c_1$ as follows:

$$\begin{aligned}
 c &= \{[(r_3 \times c_3) \cdot L] c_1 - [(r_1 \times c_1) \cdot L] c_3\} / l_v \\
 &= \{-[(r_3 \times c_1) \cdot L] c_1 + [(r_1 \times c_1) \cdot L] c_1\} / l_v \\
 &= \{-[(L \times r_3) \cdot c_1] c_1 + [(L \times r_1) \cdot c_1] c_1\} / l_v \\
 &= L \times (r_1 - r_3) / l_v = L \times (l_1x - LL) / l_v = X \times x, \tag{9a}
 \end{aligned}$$

$$\begin{aligned}
 \tau &= e_1 \times \{[(r_3 \times c_3) \cdot L] c_1 - [(r_1 \times c_1) \cdot L] c_3\} / l_v \\
 &\quad + l_1x \times [(r_1 \times c_1) \cdot L] c_3 / l_v \\
 &= e_1 \times c + x \times [(r_1 \times c_1) \cdot L] c_3 \\
 &= e_1 \times c - x \times [(L \times r_1) \cdot c_1] c_1 \\
 &= e_1 \times c - x \times (L \times r_1) = e_1 \times c - x \times (X \times r_1) \tag{9b}
 \end{aligned}$$

Let $\{v_{ri}, a_{ri} (i = 1, 2, 3)\}$ be the input (velocity, acceleration) of the parallel wrist along r_i . The formula for solving v_{ri} is represented as below:

$$v_{ri} = (\delta_i^T \quad (e_i \times \delta_i)^T) V \tag{10}$$

Let (V_{pr}, A_{pr}) be the general input velocity, the acceleration of the couple-constrained parallel wrist. Let (V, A) be the general output velocity, the acceleration of m at o . Based on the formulas for solving the displacement and the couple constrained forces, the relations of (V_{pr}, V) of the couple-constrained parallel wrist are derived from Eqs. (9a), (9b), (10) as follows:

$$\begin{aligned}
 & V_{pr} = J V, V = J^{-1} V_{pr}, V^T = V_r^T (J^{-1})^T, \\
 & V_{pr} = \begin{pmatrix} v_{r1} \\ v_{r2} \\ v_{r3} \\ 0 \\ 0 \\ 0 \end{pmatrix}, J = \begin{pmatrix} \delta_1^T & (e_1 \times \delta_1)^T \\ \delta_2^T & (e_2 \times \delta_2)^T \\ \delta_3^T & (e_3 \times \delta_3)^T \\ x^T & (x \times o)^T \\ y^T & (y \times o)^T \\ c^T & \tau^T \end{pmatrix} \tag{11a}
 \end{aligned}$$

The relations of (A_{pr}, A) of the couple-constrained parallel wrist are derived from Eqs. (11a) as follows:

$$A_{pr} = JA + J'V = JA + V^T H V, J' = V^T H, \tag{11b}$$

$$A_{pr} = \begin{pmatrix} a_{r1} \\ a_{r2} \\ a_{r3} \\ 0 \\ 0 \\ 0 \end{pmatrix}, J' = \begin{pmatrix} \delta_1^T & (e_1 \times \delta_1)^T \\ \delta_2^T & (e_2 \times \delta_2)^T \\ \delta_3^T & (e_3 \times \delta_3)^T \\ x^T & (x \times o)^T \\ y^T & (y \times o)^T \\ c^T & \tau^T \end{pmatrix}, H = \begin{pmatrix} h_1 \\ h_2 \\ h_3 \\ h_4 \\ h_5 \\ h_6 \end{pmatrix}$$

here, J and H are the 6×6 Jacobian matrix and the six layers 6×6 Hessian matrix of the couple-constrained parallel wrist, respectively; h_i ($i = 1, 2, 3$) are the 6×6 sub-matrices of H corresponding to the actuation forces f_{ai} along r_i ; (h_4, h_5) are the 6×6 sub-matrices of H corresponding to constrained forces (f_{c01}, f_{c02}) , respectively; h_6 is the 6×6 sub-matrix of H corresponding to f_{ci} ($i = 1, 3$).

In order to solve the sub-items of H in Eq. (11), several extended skew-symmetric matrices and relative formulas are derived and explained as follows.

Let ζ and $\hat{\zeta} = s(\zeta)$ be a vector and its skew-symmetric matrix, respectively. Let C be a three layers 3×3 constant matrix. Let I_k ($k = 1, 2, 3$) be the 3×3 sub-matrixes of C . The relative formulas are represented by [21].

The formulas for solving h_i ($i = 1, 2, 3$) in Eq. (11b) are derived by [22]. The formulas for solving h_4 and h_5 in Eq. (11b) are derived as follows:

$$x' = \omega \times x, x'^T = \omega^T \hat{x} = V^T \begin{pmatrix} 0 \\ \hat{x} \end{pmatrix}, (x \times o)^T = V^T \begin{pmatrix} -\hat{x} \\ \hat{x}\hat{o} \end{pmatrix}, \tag{12}$$

$$h_4 = (x'^T \quad (x \times o)^T) = \begin{pmatrix} 0 & -\hat{x} \\ \hat{x} & \hat{x}\hat{o} \end{pmatrix}, h_5 = \begin{pmatrix} 0 & -\hat{y} \\ \hat{y} & \hat{y}\hat{o} \end{pmatrix}$$

The formulas for solving h_6 in Eq. (11b) are derived as

$$c' = (X \times x)' = X \times (\omega \times x) = (0_{3 \times 3} \quad -\hat{X}\hat{x}) V, \tag{13a}$$

$$c' = (h_{c1} \quad h_{c2}) V, h_{c1} = 0_{3 \times 3}, h_{c2} = -\hat{X}\hat{x}, r'_i = v + \omega \times e_i$$

$$\tau' = (e_1 \times c)' - (x \times W)' \tag{13b}$$

$$= (\hat{c}\hat{e}_1 - \hat{e}_1\hat{X}\hat{x} - \hat{W}\hat{x} + \hat{x}\hat{X}\hat{e}_1) \omega - \hat{x}\hat{X}v = (h_{\tau1} \quad h_{\tau2}) V$$

$$W = X \times r_1, h_{\tau1} = -\hat{x}\hat{X}, \tag{13c}$$

$$h_{\tau2} = \hat{c}\hat{e}_1 - \hat{e}_1\hat{X}\hat{x} - \hat{w}\hat{x} + \hat{x}\hat{X}\hat{e}_1,$$

$$((c')^T \quad (\tau')^T) = V^T h_6, h_6 = \begin{pmatrix} h_{c1}^T & h_{\tau1}^T \\ h_{c2}^T & h_{\tau2}^T \end{pmatrix}$$

3. Workspace of couple-constrained parallel wrist with three flexible fingers

The parameters of the parallel wrist are listed in Table I.

The reachable workspace of the gripper is an important index to evaluate its operation performance. A reachable workspace of the gripper is constructed, see Fig. 3.

Since the couple-constrained parallel wrist has a symmetry structure in OYZ plane, its reachable workspace is also symmetry in OZX plane. Let $\{r_{imax}, r_{imin}, \Delta r_i$ ($i = 1, 2, 3$) $\}$ be (the maximum extension, the maximum extension, and the increment from r_{imin} to r_{imax}) of r_i , respectively. Let $\{r_{wrjmax}, r_{wrjmin}, \Delta r_{wrj}$ ($j = 1, 2, 3$) $\}$ be (the maximum extension, the maximum extension and the increment from r_{wrjmin} to

Table I. Parameters of couple-constrained parallel wrist.

| Parameters and symbols | values, unit |
|--|-------------------------------|
| s_m, s_B sides of m and B | 150/3 ^{1/2} , 250 mm |
| a_{r1}, a_{r2}, a_{r3} input accelerations | 2, 1, 1 mm/s ² |
| initial length of $r_i, (i = 1, 2, 3)$ | 360 mm |
| r_i input length range input | 360 → 500 mm |
| increment Δr_i of r_i | 10 mm |
| μ, η, f, t | 0, 1, 0, 0 |
| the j th finger force f_{wj} | [1 2 3] ^T N |
| the j th finger torque t_{wj} | [4 5 6] ^T N · m |
| $m_o, {}^u I_u$ | 1 kg, I kg·m ² |

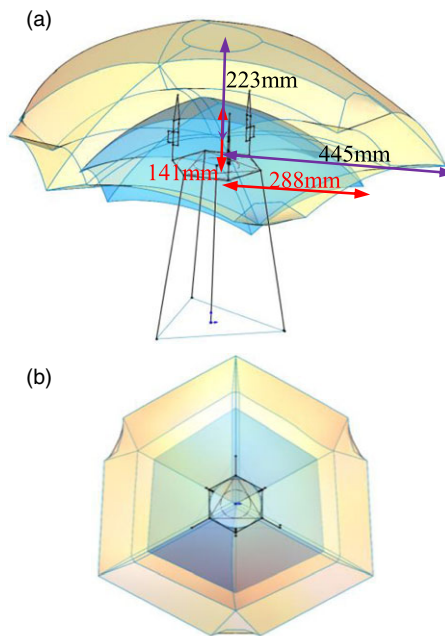


Figure 3. Reachable workspaces of couple-constrained parallel wrist with three flexible fingers at fingertips. A isometric view with dimensions (a). A top view (b).

r_{wrjmax}) of r_{wrj} , respectively. In the light of the basic parameters listed in Table I, the reachable workspace W of the gripper is constructed using Matlab and is transformed into Solidwork using CAD variation geometry [23]. It is known from Fig. 3 that the workspaces of the three finger equivalent mechanisms at the fingertips in the developed gripper are quite large.

4. Dynamics model of couple-constrained parallel wrist with three flexible fingers

The kinematics of moving limbs r_i are the pre-conditions of the dynamics analysis of the couple-constrained parallel wrist with three flexible fingers. Since the kinematics of r_i are quite complicated, the derivation kinematics formulas of r_i are explained in Appendix A. A dynamics model of the gripper is shown in Fig. 4. Some symbols for establishing the dynamics model are explained as follows.

Let g_i be the piston rod as $g = p$ or the cylinder as $g = q$ in r_i . Each of the limbs $r_i (i = 0, 1, 2, 3)$ is composed of a piston rod with its mass center p_i and a cylinder with its mass center q_i . Let a_{gi} be the

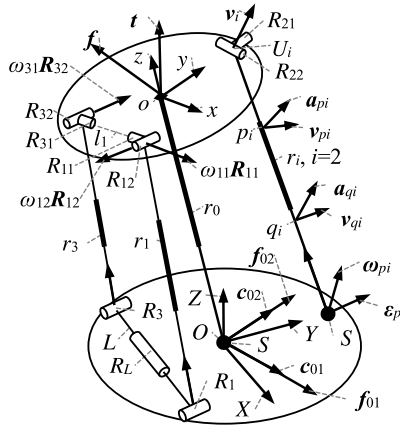


Figure 4. Dynamics model of limbs r_i ($i = 0, 1, 2, 3$).

translational acceleration of the moving link g_i in r_i at its mass center in $\{B\}$. Let ϵ_i angular velocity acceleration of r_i . Let J_{gi} ($g = p, q$) be the Jacobian matrix of the moving link g_i in r_i . Let V_{gi} and A_{gi} be the general velocity and the general acceleration of g_i in r_i ($i = 0, 1, 2, 3$). The formulas for solving $\{a_{gi}, \epsilon_i, J_{gi} (g = p, q), V_{gi}, A_{gi}\}$ are derived in Appendix A.

Let f_u, t_u, m_u, I_u, G_u ($u = o, p_i, q_i; i = 0, 1, 2, 3$) be the inertial force, inertial torque, the mass, the inertial moment, the gravity of the moving links at their mass centers in $\{B\}$, respectively. Let (f, t) be the working-load wrench applied on m_p at o . Let (f_d, t_d) be the damping force and torque applied on m_p at o , respectively. Let μ be a damping coefficient. The formulas for solving $(f_u, t_u, G_u, I_u, f_d, t_d)$ are represented as

$$\begin{aligned} \begin{pmatrix} f_u \\ t_u \end{pmatrix} &= -M_u A_u - \begin{pmatrix} \mathbf{0} \\ \omega_u \times (I_u \omega_u) \end{pmatrix}, M_u = \begin{pmatrix} m_u I & 0 \\ 0 & I_u \end{pmatrix}, \\ G_u &= m_u g, f_u = -m_u a_u, \{u = m, p_i, q_i, (i = 0, 1, 2, 3)\}, \\ t_u &= -I_u \epsilon_u - \omega_u \times (I_u \omega_u), f_d = -\mu v, t_d = -\mu \omega \end{aligned} \tag{14}$$

Let f_{ai} ($i = 1, 2, 3$) be the scalar of the input actuation force along r_i . Let f_j ($j = 1, 2, 3$) be the scalar of the input actuation forces of the j th finger. Let f_c be the scalar of the constrained force exerted on m_p of the parallel wrist, see Fig. 3. Let F_r be the general actuation/constrained forces of the developed parallel wrist and the three fingers. Let V_f be the general input velocity of the three finger mechanisms. Let V_r be the general input velocity of the developed parallel wrist and the three fingers. They are represented in $\{B\}$ based on Eq. (11) as follows:

$$\begin{aligned} V_r &= \begin{pmatrix} V_{pr} \\ V_f \end{pmatrix}, F_r = \begin{pmatrix} F_{pr} \\ F_f \end{pmatrix}, V_f = \begin{pmatrix} y'_1 \\ y'_2 \\ y'_3 \end{pmatrix}, F_f = \begin{pmatrix} f_1 \\ f_2 \\ f_3 \end{pmatrix}, \\ V_{pr} &= (v_{r1} \ v_{r2} \ v_{r3} \ 0 \ 0 \ 0)^T, \\ F_{pr} &= (f_{a1} \ f_{a2} \ f_{a3} \ f_{c01} \ f_{c02} \ f_c)^T \end{aligned} \tag{15}$$

Let (f_{wj}, t_{wj}) be the working-load wrench applied on the j th fingertip w_j . Let V_{wj} be the general velocity of the j th fingertip w_j in $\{B\}$. When ignoring the friction of all the joints in the mechanism, f and t are applied onto m_p , based on the principle of virtual work, a power equation is derived as

$$\begin{aligned} V_r^T F_r + V^T \begin{pmatrix} f + f_o + g_o + f_d \\ t + t_o + t_d \end{pmatrix} + \sum_{j=1}^3 V_{wj}^T \begin{pmatrix} f_{wj} \\ t_{wj} \end{pmatrix} \\ + \sum_{i=0}^3 \left(V_{pi}^T \begin{pmatrix} f_{pi} + g_{pi} \\ t_{pi} \end{pmatrix} + V_{qi}^T \begin{pmatrix} f_{qi} + g_{qi} \\ t_{qi} \end{pmatrix} \right) &= 0 \end{aligned} \tag{16}$$

here, the items from the left to the right in Eq. (16) are the powers generated by F_r , by (f_o, t_o, g_o) of m and (f, t) and (f_d, t_d) applied on m_p , by (f_{wi}, t_{wi}) , and by (f_L, t_L, g_L) , respectively.

A formula for solving V_{wj}^T is represented as follows:

$$V_{wj}^T = V_{pr}^T (J_{wj} J^{-1})^T + V_f^T ({}^B J^T J_{wrj} J_{ej})^T \tag{17}$$

here, V_{wj}^T is derived (Lu, et al. 2021).

The relations V_{pr} and V are represented based on Eqs. (11), (16) as follows:

$$\begin{aligned} V_r^T F_r &= V_{pr}^T F_{pr} + V_f^T F_f, V^T = V_{pr}^T (J^{-1})^T, \\ V_{gi}^T &= V^T J_{gi}^T = V_{pr}^T (J^{-1})^T J_{gi}^T, (g = p, q) \end{aligned} \tag{18}$$

Considering the friction of the joints in the mechanism, the efficiency ($\eta \leq 1$) of the developed gripper can be added here. Thus, the formulas for solving the general dynamic actuation forces and the dynamic constrained forces are derived by substitute Eqs. (17), (18) into Eq. (16) as

$$F_f = -\frac{1}{\eta} \sum_{j=1}^3 ({}^B J^T J_{wrj} J_{Ej})^T \begin{pmatrix} f_{wj} \\ t_{wj} \end{pmatrix}, \tag{19a}$$

$$\begin{aligned} F_{pr} = - (J^{-1})^T &\left\{ \frac{1}{\eta} \left(\begin{pmatrix} f \\ t \end{pmatrix} - \mu V - M_o A + \begin{pmatrix} m_o g \\ -\omega_o \times (I_o \omega_o) \end{pmatrix} \right) \right. \\ &+ \sum_{i=0}^3 J_{pi}^T \left(-M_{pi} A_{pi} + \begin{pmatrix} m_{pi} g \\ -\omega_i \times (I_{pi} \omega_i) \end{pmatrix} \right) \\ &\left. + \sum_{i=0}^3 J_{qi}^T \left(-M_{qi} A_{qi} + \begin{pmatrix} m_{qi} g \\ -\omega_i \times (I_{qi} \omega_i) \end{pmatrix} \right) + \sum_{j=1}^3 (J_{wj})^T \begin{pmatrix} f_{wj} \\ t_{wj} \end{pmatrix} \right\} \end{aligned} \tag{19b}$$

The formulae for solving the dynamic couple-constrained forces f_{ci} ($i = 1, 3$) and the dynamic constrained torque t_c exerted on to L are derived by utilizing Eqs. (7), (19b) as follows:

$$\begin{aligned} f_c &= f_{c1} + f_{c3}, f_{c1} = \frac{f_c}{1+k}, f_{c3} = f_c - f_{c1}, \\ t_c &= (r_1 \times f_{c1} c_1) \cdot X, k = (r_1 \times c_1) \cdot x / [(r_3 \times c_1) \cdot x] \end{aligned} \tag{20}$$

5. Theoretical solutions of kinematics/dynamics

A program is compiled using Matlab based on the theoretical formulas in Sections 2, 4 and Appendix A. Theoretical kinematics solutions of m_p of parallel wrist are solved, see Fig. 5.

The dynamic actuation forces f_{ai} ($i = 1, 2, 3$) of the parallel wrist are solved, see Fig. 6a. The dynamic actuation forces f_j ($j = 1, 2, 3$) of the fingers are solved, see Fig. 6b. The dynamic constrained forces f_{c0i} ($i = 1, 2$) of the parallel wrist exerted on r_0 are solved, see Fig. 6c. The dynamic constrained forces f_{ci} ($i = 1, 3$) of the parallel wrist exerted on L and the dynamic constrained torque t_c are solved, see Fig. 6d.

In order to verify the correctness of the theoretical solutions of the gripper, an equivalent simulation mechanism of the gripper with three fingers and a logical block of RPR-type actuation limbs r_1 and r_3 , a logical block of SPU type actuation limb r_2 are constructed, respectively, using Matlab/Simulink/Mechanics, see Appendix B. The absolute errors Δx between the maximum theoretical solutions x and the maximum simulation solutions x_s are listed in Table II and Table A1. It is known from Table II that the theoretical solutions coincide with that of the simulation mechanism. Hence, the derived formulas in Sections 2, 3, and Appendix A are correct.

6. Experiment of prototype of couple-constrained parallel wrist with three flexible fingers

Two poses of prototype of couple-constrained parallel wrist with three flexible fingers are shown in Fig. 7a, b.

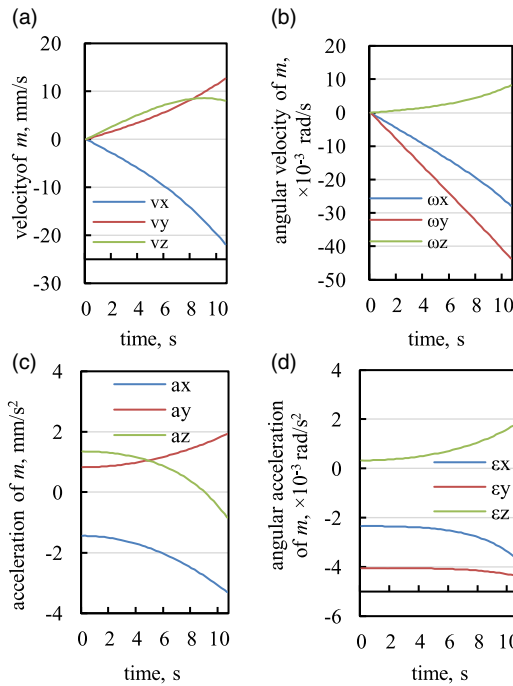


Figure 5. Theoretical kinematics solutions of the moving platform m_p of couple-constrained parallel wrist with three force flexible fingers.

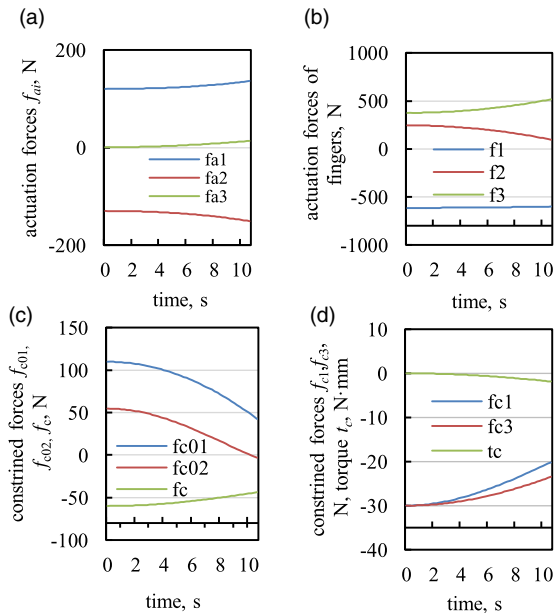


Figure 6. Theoretical dynamics solutions of dynamic actuation forces, the dynamic constrained forces, and torque of parallel wrist.

Table II. Absolute errors $\Delta x = \text{abs}(x - x_s)$ between the maximum theoretical solutions x and the maximum simulation solutions x_s .

| Δv_x | Δv_y | Δv_z | Δa_x | Δa_y | Δa_z | $\Delta \omega_x$ | $\Delta \omega_y$ | $\Delta \omega_z$ |
|-------------------------|-------------------------|------------------------|-------------------------|-------------------------|-------------------------|-------------------------|-------------------------|------------------------|
| -4.33×10^{-13} | 2.53×10^{-13} | 1.00×10^{-13} | -5.07×10^{-12} | -4.76×10^{-12} | -1.31×10^{-12} | -7.18×10^{-13} | -1.22×10^{-12} | 9.87×10^{-14} |
| $\Delta \varepsilon_x$ | $\Delta \varepsilon_y$ | $\Delta \varepsilon_z$ | Δf_{a1} | Δf_{a2} | Δf_{a3} | Δf_{c01} | Δf_{c02} | Δf_c |
| 8.00×10^{-12} | -1.05×10^{-12} | 8.60×10^{-14} | -2.47×10^{-7} | 4.49×10^{-7} | -2.31×10^{-7} | -4.12×10^{-5} | 1.36×10^{-6} | 9.50×10^{-8} |

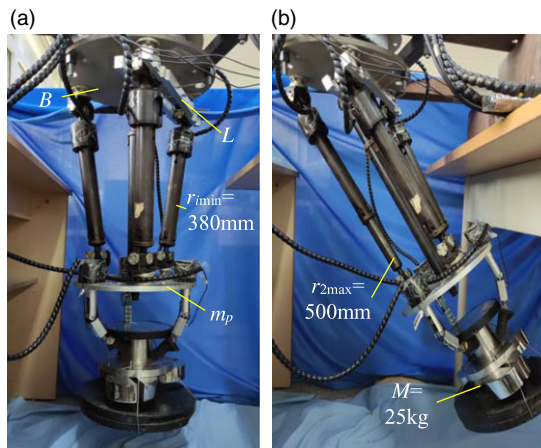


Figure 7. Prototype of couple-constrained parallel wrist with three flexible fingers for grabbing object $M = 25 \text{ kg}$ in two poses as $r_i = r_{\text{imin}}$ ($i = 1, 2, 3$) (a), and as $r_2 = r_{2\text{max}}$, $r_1 = r_3 = r_{\text{imin}}$ (b).

Let r_{imin} ($i = 1, 2, 3$) and r_{imax} be the minimum and maximum extension of actuation limbs r_i . Let M be the mass of the grabbed object. M is increased to 25 kg, see Fig. 7b. Let f_{si} be measured forces of sensor of fingers i . A measured system is built to measure f_{si} as grabbing object with different masses, see Fig. 8a. As grabbing object with $M = 14 \text{ kg}$, the measured results of f_{si} are shown in Fig. 8b.

It is known from the experiments the developed prototype of couple-constrained parallel wrist with three measuring force flexible fingers that:

1. A heavy workload $M = 25 \text{ kg}$ can be grabbed and moved in the large workspace, see Fig. 3 and Fig. 7b.
2. A large grabbing impact can be reduced greatly using a pre-pressured spring installed in the finger, see Fig. 8b.
3. The measured forces f_{si} are varied smoothly as grabbing the object with constant mass and moving smoothly. (f_{s1}, f_{s2}, f_{s3}) are different with each other, which are dependent on the grasping pose and the manufacturing precise of the finger, see Fig. 8b.

The measuring force flexible finger is formed by a screw motor 1 and a seat 2 fixed onto m_p , a nut 3, a sensor 4, a sleeve 5, a spring 6 and a inner sleeve in sleeve, a fingertip link 7, a long slice 8, a short slice 9, see Fig. 9. A big heavy tub and an egg 10 can be grabbed, see Fig. 9.

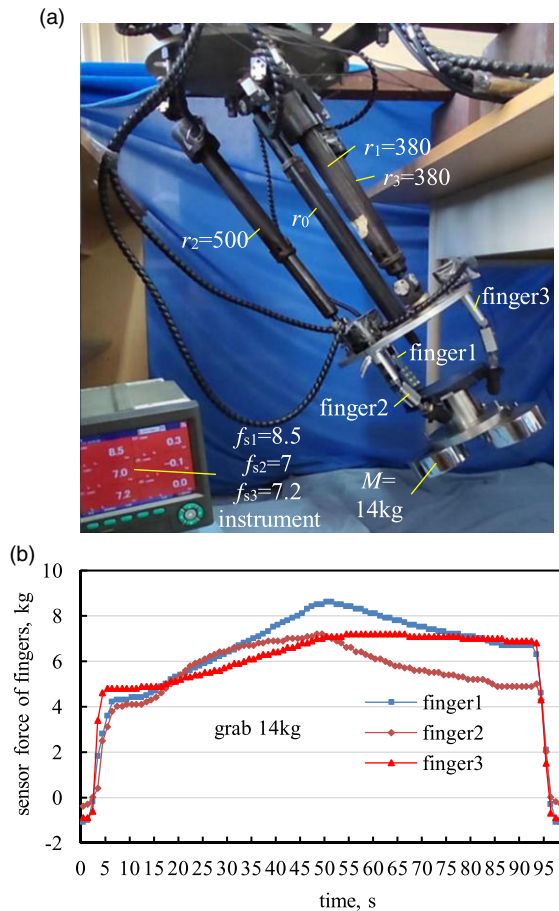


Figure 8. Measured system of sensor forces f_{s_i} of fingers in developed gripper as grabbing object with different masses (a), Measured results of f_{s_i} as grabbing object with $M = 14\text{ kg}$ (b).

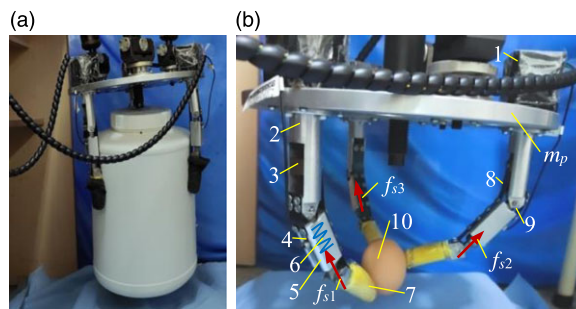


Figure 9. A big heavy tub (a) and a easy breakage egg (b) grabbed by couple-constrained parallel wrist with three flexible fingers.

7. Conclusions

The developed novel couple-constrained parallel wrist has three DOFs and quite large workspace which is benefited to increase the dexterity of the gripper.

The couple-constrained parallel wrist with three measuring force flexible fingers can be used to grab the heavy objects with various shapes or large volume. It also can be used to grab the small and easy

breakage object. A large grabbing impact can be reduced greatly using a pre-pressured spring installed in the finger.

The theoretical solutions of the kinematics and dynamics of the couple-constrained parallel wrist with three measuring force flexible fingers are verified to be correct by its simulation mechanism. These kinematics and dynamics models of the developed couple-constrained parallel wrist with three measuring force flexible fingers provide a theoretical foundation for analysis of the dynamics and stiffness of other grippers and their control.

Further study should be conducted on the synthesis and optimization of the kinematic parameters of the overall gripper mechanism in order to increase the grabbing capability and the dexterity of the gripper.

Author contributions. Yang Lu and Yi Lu conceived and designed the study and experiment. Zefeng Chang conducted data gathering and formulas derivation, and simulation verification. Yi Lu wrote the article.

Financial support. The authors are grateful to Natural Science Foundation (grant number E2020203010) of Hebei, China.

Competing interest. We have no potential conflicts of interest.

Ethical standard. Not applicable, as this paper does not include any human and/or animal experimentation.

References

- [1] M. Honarpardaz, M. Tarkian and J. Olvander, "Finger design automation for industrial robot grippers: a review," *Robot. Auton. Syst.* **87**, 104–119 (2017).
- [2] Z. Kappassov, J. Corrales and V. Perdereau, "Tactile sensing in dexterous robot hands - review," *Robot. Auton. Syst.* **74**, 195–220 (2015).
- [3] G. Li, L. Cheng, Z. Gao, X. Xia and J. Jiang, "Development of an untethered adaptive thumb exoskeleton for delicate rehabilitation assistance," *IEEE Trans. Robot.* **38**(6), 3514–3529 (2022).
- [4] G. Li, L. Cheng and N. Sun, "Design, manipulability analysis and optimization of an index finger exoskeleton for stroke rehabilitation," *Mech. Mach. Theory* **167**, 104526 (2022).
- [5] J. J. Craig. *Introduction to Robotics* (Addison- Wesley Publishing Co, New York, 1989).
- [6] Z. Huang, Q. Li and H. Ding. *Theory of Parallel Mechanisms* (Springer, New York, 2013).
- [7] D. Zhang. *Parallel Robotic Machine Tools* (Springer, New York Dordrecht Heidelberg London, 2010).
- [8] Y. Pan and F. Gao, "Position model computational complexity of walking robot with different parallel leg mechanism topology patterns," *Mech. Mach. Theory* **107**, 324–337 (2017).
- [9] X. Kong and C. M. Gosselin, "Type synthesis of three- degree- of-freedom spherical parallel manipulators," *Int. J. Robot. Res.* **23**(3), 237–245 (2004).
- [10] M. Ebrahim, "A survey of bio-inspired robotics hands implementation: New directions in dexterous manipulation," *Robot. Auton. Syst.* **61**(5), 517–544 (2013).
- [11] B. Spencer, O. Rina, B. Andrew, B. Andrew, D. Eric and P. Aaron, "Design and testing of the JPL-Nautilus Gripper for deep-ocean geological sampling," *J. Field Robot.* **37**(6), 972–986 (2020).
- [12] X. Jin, Y. Fang and D. Zhang, "Design of dexterous hands based on parallel finger structures," *Mech. Mach. Theory* **152**, 103952 (2020).
- [13] X. Jin, Y. Fang and D. Zhang, "Synthesis of 3-[P][S] parallel mechanism-inspired multimode dexterous hands with parallel finger structure," *J. Mech. Des.* **142**(8), Article No. 083301 (2020).
- [14] J. He, J. Li and Z. Sun, "Kinematic design of a serial-parallel hybrid finger mechanism actuated by twisted-and-coiled polymer," *Mech. Mach. Theory* **152**, Article No. 103951 (2020).
- [15] Y. Zheng, B. Wu and Y. Chen, "Design and validation of cable-driven hyper-redundant manipulator with a closed- loop puller-follower controller," *Mechatronics* **78**, Article No. 102605 (2021).
- [16] Z. Li, Z. Hou and Y. Mao, "The development of a two-finger dexterous bionic hand with three grasping patterns-nwafu hand," *J. Bionic Eng.* **17**(4), 718–731 (2020).
- [17] M. Isaksson, C. M. Gosselin and K. Marlow, "An introduction to utilizing the redundancy of a kinematically redundant parallel manipulator to operate a gripper," *Mech. Mach. Theory* **101**, 50–59 (2016).
- [18] R. Geng, J. Mills and Z. Yao, "Design and analysis of a novel 3-DOF spatial parallel microgripper driven by LUMs," *Robot. Comput-Integr. Manuf.* **42**, 147–155 (2016).
- [19] C. Han, J. Kim, J. W. Kim and C. P. Fran, "Kinematic sensitivity analysis of the 3-UPU parallel mechanism," *Mech. Mach. Theory* **37**(8), 787–798 (2002).
- [20] Y. Lu, Z. F. Chang and Y. Lu, "Development and kinematics/statics analysis of rigid-flexible-soft hybrid finger mechanism with standard force sensor," *Robot. Comput. Integr. Manuf.* **67**, Article No. 101978 (2021).

[21] Y. Lu, N. J. Ye and Z. F. Chang, "Derivation of general acceleration and hessian matrix of kinematic limbs in parallel manipulator by extended skew symmetric matrixes," *Arch. Comput. Method Eng.* **28**(4), 3035–3047 (2021).
 [22] Y. Lu and B. Hu, "Unification and simplification of velocity/ acceleration of limited-dof parallel manipulators with linear active legs," *Mech. Mach. Theory* **43**(9), 1112–1128 (2008).
 [23] Y. Lu, Y. Shi and B. Hu, "Solving reachable workspace of some parallel manipulators by computer-aided design variation geometry," *Proc. Inst. Mech. Eng. C J. Mech. Eng. Sci.* **222**(4), 1773–1781 (2008).

Appendix A

A. Kinematics of moving limbs r_i

The kinematic models of the moving limbs r_i are shown in Fig. 3. Let v_i ($i = 1, 2, 3$) be the translational velocity of r_i at point b_i in $\{B\}$. Let (ω_i, ϵ_i) be the angular (velocity and acceleration) of r_i in $\{B\}$. g_i may be the piston rod as $g = p$ or the cylinder as $g = q$ in r_i . The formulas of $(r_i, e_i, v, \omega, v_i, \omega_i, v_i)$ can be represented as follows:

$$v_i = v_{ri}\delta_i + \omega_i \times r_i, v_i = v + \omega \times e_i, v_i - v_{ri}\delta_i = \omega_i \times r_i \tag{A1}$$

The kinematics/statics formulas of the flexible finger have been derived by [21]. The kinematics formulas of the moving limbs r_i ($i = 0, 1, 2, 3$) are derived as follows.

A.1. Angular velocity/acceleration of actuation limbs r_i

Cross multiply both sides of the first formula in Eq. (A1) in the right by r_i , it leads to

$$\begin{aligned} \delta_i \times v_i &= \delta_i \times v_{ri}\delta_i + r_i\delta_i \times (\omega_i \times \delta_i) \\ &= r_i\delta_i \times (\omega_i \times \delta_i) = r_i\omega_i - r_i(\delta_i \cdot \omega_i)\delta_i \end{aligned} \tag{A2}$$

The upper ends of r_i ($i = 1, 2, 3$) are connected with m by U_i at b_i , U_i is formed by two crossed revolute joints R_{ij} ($j = 1, 2$), and $(R_{i1} \perp R_{i2}, R_{i1} \perp z, R_{i2} \perp r_i, R_{i1} \parallel R_{31})$ are satisfied. Let R_{ij} be the unit vector of R_{ij} . The angular velocities ω_i ($i = 1, 2, 3$) of r_i are satisfied as follows:

$$\begin{aligned} \omega_i + \theta'_{i1}R_{i1} + \theta'_{i2}R_{i2} &= \omega, \\ R_{i2} &= R_{i1} \times r_i / |R_{i1} \times r_i|, (i = 1, 2, 3) \end{aligned} \tag{A3}$$

here, θ'_{ij} ($i = 1, 2, 3; j = 1, 2$) are the scalar angular speeds of r_i about R_{ij} .

Cross multiply both sides of Eq. (A3) in the right by r_i , it leads to

$$\begin{aligned} \omega \times r_i - \theta'_{i1}R_{i1} \times r_i - \theta'_{i2}R_{i2} \times r_i &= \omega_i \times r_i \\ &= v_i - v_{ri}\delta_i = v_i - (v_i \cdot \delta_i)\delta_i = -\hat{\delta}_i^2(v + \omega \times e_i) \end{aligned} \tag{A4}$$

Dot multiply both sides of Eq. (A4) in the right by R_{i1} and R_{i2} , respectively, it leads to

$$\begin{aligned} (\omega \times r_i) \cdot R_{i1} - (\theta'_{i2}R_{i2} \times r_i) \cdot R_{i1} &= \hat{\delta}_i^2(-v + \hat{e}_i\omega) \cdot R_{i1}, \\ (\omega \times r_i) \cdot R_{i2} - (\theta'_{i1}R_{i1} \times r_i) \cdot R_{i2} &= \hat{\delta}_i^2(-v + \hat{e}_i\omega) \cdot R_{i2} \end{aligned} \tag{A5}$$

The formulas of θ'_{i1} and θ'_{i2} are derived from Eq. (A5) as

$$\begin{aligned} \theta'_{i1} &= \left[-(\hat{r}_i R_{i2}) \cdot \omega - \hat{\delta}_i^2(v - \hat{e}_i\omega) \cdot R_{i2} \right] / d_{i1}, \\ \theta'_{i2} &= \left[(\hat{r}_i R_{i1}) \cdot \omega + \hat{\delta}_i^2(v - \hat{e}_i\omega) \cdot R_{i1} \right] / d_{i1}, \\ d_{i1} &= (R_{i1} \times R_{i2}) \cdot r_i \end{aligned} \tag{A6}$$

Substitute Eqs. (A6) for Eq. (A5), a formula for solving ω_i is derived from Eq. (A3) as follows:

$$\begin{aligned} \omega_i &= \omega - R_{i1}\theta'_{i1} - R_{i2}\theta'_{i2} \\ &= \omega + R_{i1} \left[R_{i2}^T (\omega \times r_i) + R_{i2}^T \hat{\delta}_i^2 (v - \hat{e}_i \omega) \right] / d_{i1} \\ &\quad - R_{i2} \left[R_{i1}^T (\omega \times r_i) + R_{i1}^T \hat{\delta}_i^2 (v - \hat{e}_i \omega) \right] / d_{i1}, \\ \omega_i &= \omega - d_{i2} \left[(r_i \hat{\delta}_i \omega) - \hat{\delta}_i^2 (v - \hat{e}_i \omega) \right] / d_{i1}, \\ d_{i2} &= R_{i1} R_{i2}^T - R_{i2} R_{i1}^T, d_{i1} = r_i \cdot (R_{i1} \times R_{i2}) \end{aligned} \tag{A7}$$

Eq. (A7) is simplified as follows:

$$\begin{aligned} \omega_i &= (J_{\omega i})_{3 \times 6} V, J_{\omega i} = (J_{\omega i1} \quad J_{\omega i2}) / d_{i1}, \\ J_{\omega i1} &= d_{i2} \hat{\delta}_i^2, R_{i2} = (R_{i1} \times r_i) / |R_{i1} \times r_i|, \\ J_{\omega i2} &= d_{i1} I - d_{i2} (\hat{r}_i + \hat{\delta}_i^2 \hat{e}_i) = d_{i1} I - d_{i2} \hat{r}_i - J_{\omega i1} \hat{e}_i \end{aligned} \tag{A8}$$

The items $\{d_{i2}, r_i \cdot (R_{i1} \times R_{i2})', d_{i2} \hat{r}_i', d_{i1}'\}$ for solving ε_i are derived as follows:

$$\begin{aligned} R_{i1} \cdot R_{i2} &= 0, R'_{i1} = \omega \times R_{i1}, R'_{i2} = \omega_i \times R_{i2}, \\ d_{i2} &= R_{i1} R_{i2}^T - R_{i2} R_{i1}^T = s (R_{i2} \times R_{i1}), R_{i2} \cdot r_i = 0, \\ [(R_{i2} \times R_{i1})']^T &= (R'_{i2} \times R_{i1} + R_{i2} \times R'_{i1})^T \\ &= (\omega_i \cdot R_{i1}) R_{i2}^T - (\omega \cdot R_{i2}) R_{i1}^T = \omega_i^T R_{i1} R_{i2}^T - \omega^T R_{i2} R_{i1}^T, \end{aligned} \tag{A9}$$

$$\begin{aligned} r_i \cdot (R_{i1} \times R_{i2})' &= -r_i \cdot (R_{i2} \times R_{i1})' \\ &= -(\omega_i \cdot R_{i1}) (r_i \cdot R_{i2}) + (R_{i2} \cdot \omega) (r_i \cdot R_{i1}) \\ &= \omega^T R_{i2} (r_i \cdot R_{i1}), d_{i2} \hat{r}_i' = -(r_i')^T (d_{i2} C) = -V^T \left(\hat{e}_i \right) (d_{i2} C), \\ d_{i1}' &= [(R_{i1} \times R_{i2}) \cdot r_i]' = r_i' \cdot (R_{i1} \times R_{i2}) + r_i \cdot (R_{i1} \times R_{i2})' \\ &= (v + \omega \times e_i)^T (R_{i1} \times R_{i2}) + \omega^T R_{i2} (r_i \cdot R_{i1}) \\ &= V^T \left[\left(\hat{e}_i \right) (R_{i1} \times R_{i2}) + \left(\mathbf{0} \right) R_{i2} (r_i \cdot R_{i1}) \right] \end{aligned}$$

The items $\{d'_{i2}, d_{i2} \hat{\delta}_i', d_{i2} \hat{\delta}_i^2 \hat{e}_i', d_{i2} (\hat{\delta}_i^2)'\}$ for solving ε_i are derived from Eq. (A9) as follows:

$$\begin{aligned} d'_{i2} &= s (R_{i2} \times R_{i1})' = [(R_{i2} \times R_{i1})']^T C \\ &= [(\omega_i^T R_{i1}) R_{i2}^T - (\omega^T R_{i2}) R_{i1}^T] C = V^T \left\{ \left[(J_{\omega i}^T R_{i1}) R_{i2}^T - \left(\mathbf{0} \right) R_{i2} R_{i1}^T \right] C_e \right\}, \\ d_{i2} \hat{\delta}_i' &= -(\delta_i')^T d_{i2} C = \frac{v^T}{r_i} \left(\hat{e}_i \hat{\delta}_i^2 \right) (d_{i2} C), \\ d_{i2} \hat{\delta}_i^2 \hat{e}_i' &= -(e_i')^T [(d_{i2} \hat{\delta}_i^2) C] = -V^T \left(\hat{e}_i \right) [(d_{i2} \hat{\delta}_i^2) C], \\ d_{i2} (\hat{\delta}_i^2)' &= d_{i2} (\hat{\delta}_i' \hat{\delta}_i + \hat{\delta}_i \hat{\delta}_i') = -(\delta_i')^T [d_{i2} C \hat{\delta}_i + (d_{i2} \hat{\delta}_i) C] \\ &= V^T \left(\hat{e}_i \hat{\delta}_i^2 \right) \frac{[d_{i2} C \hat{\delta}_i + (d_{i2} \hat{\delta}_i) C]}{r_i} \end{aligned} \tag{A10}$$

Next, the formulas for solving $\boldsymbol{\varepsilon}_i$ are derived from Eqs. (A9) and (A10) as follows:

$$\begin{aligned}
 \boldsymbol{\varepsilon}_i &= \boldsymbol{\omega}'_i = \mathbf{J}_{\omega i} \mathbf{A} + \mathbf{J}'_{\omega i} \mathbf{V}, \mathbf{J}'_{\omega i} = [(\mathbf{J}_{\omega i 1} \quad \mathbf{J}_{\omega i 2}) - d'_{i1} \mathbf{J}_{\omega i}] / d_{i1} = \mathbf{V}^T \mathbf{H}_{\omega i}, \\
 \mathbf{J}'_{\omega i 1} &= (d_{i2} \hat{\boldsymbol{\delta}}_i^2)' = d'_{i2} \hat{\boldsymbol{\delta}}_i^2 + d_{i2} (\hat{\boldsymbol{\delta}}_i^2)' = \mathbf{V}^T \mathbf{h}_{\omega i 1}, \\
 \mathbf{h}_{\omega i 1} &= \left(\mathbf{J}_{\omega i}^T \mathbf{R}_{i1} \mathbf{R}_{i2}^T - \begin{pmatrix} \mathbf{0} \\ \mathbf{R}_{42} \mathbf{R}_{41}^T \end{pmatrix} \right) \mathbf{C}_e \hat{\boldsymbol{\delta}}_i^2 + \begin{pmatrix} \hat{\boldsymbol{\delta}}_i^2 \\ \hat{\boldsymbol{e}}_i \hat{\boldsymbol{\delta}}_i^2 \end{pmatrix} \frac{(d_{i2} \mathbf{C}) \hat{\boldsymbol{\delta}}_i + (d_{i2} \hat{\boldsymbol{\delta}}_i) \mathbf{C}}{r_i} \\
 \mathbf{J}'_{\omega i 2} &= (d_{i1} \mathbf{I} - d_{i2} \hat{\boldsymbol{r}}_i - \mathbf{J}_{\omega i 1} \hat{\boldsymbol{e}}_i)' \\
 &= d'_{i1} \mathbf{I} - d'_{i2} \hat{\boldsymbol{r}}_i - d_{i2} \hat{\boldsymbol{r}}_i' - \mathbf{J}_{\omega i 1} \hat{\boldsymbol{e}}_i' - \mathbf{J}'_{\omega i 1} \hat{\boldsymbol{e}}_i = \mathbf{V}^T \mathbf{h}_{\omega i 2}, \\
 \mathbf{h}_{\omega i 2} &= \begin{pmatrix} \mathbf{I} \\ \hat{\boldsymbol{e}}_i \end{pmatrix} [(\mathbf{R}_{i1} \times \mathbf{R}_{i2}) \mathbf{I} + d_{i2} \mathbf{C}] + \begin{pmatrix} \mathbf{0} \\ \mathbf{I} \end{pmatrix} \mathbf{R}_{i2} (r_i \cdot \mathbf{R}_{i1}) \mathbf{I} \\
 &\quad - \left[(\mathbf{J}_{\omega i}^T \mathbf{R}_{i1}) \mathbf{R}_{i2}^T - \begin{pmatrix} \mathbf{0} \\ \mathbf{R}_{i2} \mathbf{R}_{i1}^T \end{pmatrix} \right] \mathbf{C}_e \hat{\boldsymbol{r}}_i + \begin{pmatrix} \mathbf{0} \\ \hat{\boldsymbol{e}}_i \end{pmatrix} (\mathbf{J}_{\omega i 1} \mathbf{C}) - \mathbf{h}_{\omega i 1} \hat{\boldsymbol{e}}_i, \\
 \mathbf{H}_{\omega i} &= \frac{1}{d_{i1}} \left\{ (\mathbf{h}_{\omega i 1} \quad \mathbf{h}_{\omega i 2}) - \left[\begin{pmatrix} \mathbf{I} \\ \hat{\boldsymbol{e}}_i \end{pmatrix} (\mathbf{R}_{i1} \times \mathbf{R}_{i2}) + \begin{pmatrix} \mathbf{0} \\ \mathbf{I} \end{pmatrix} \mathbf{R}_{i2} (r_i \cdot \mathbf{R}_{i1}) \right] \mathbf{J}_{\omega i} \right\}
 \end{aligned}
 \tag{A11}$$

$\mathbf{H}_{\omega i}$ is the 3×6 Hessian matrix mapped from \mathbf{V} to $\boldsymbol{\varepsilon}_i$.

A.2. Translational velocity and acceleration of r_i

Each of the limbs r_i ($i = 1, 2, 3$) is composed of a piston rod with its mass center p_i and a cylinder with its mass center q_i . Let \mathbf{v}_{gi} and \mathbf{a}_{gi} be, respectively, the translational velocity and the acceleration of the moving link g_i in r_i at its mass center in $\{B\}$, $g = p$ for the piston rod, $g = q$ for the cylinder. Let r_i be the distance from B_i to b_i . Let l_{pi} be the distance from b_i to p_i . Let l_{qi} be the distance from B_i to q_i . The formulas for solving \mathbf{v}_{gi} are derived as follows:

$$\begin{aligned}
 \mathbf{v}_{pi} &= v_{ri} \boldsymbol{\delta}_i + \boldsymbol{\omega}_i \times (r_i - l_{pi}) \boldsymbol{\delta}_i = \mathbf{J}_{vpi} \mathbf{V}, \\
 \mathbf{J}_{vpi} &= \boldsymbol{\delta}_i \boldsymbol{\delta}_i^T (\mathbf{I} \quad -\hat{\boldsymbol{e}}_i) - (r_i - l_{pi}) \hat{\boldsymbol{\delta}}_i \mathbf{J}_{\omega i}, \\
 \mathbf{v}_{qi} &= \boldsymbol{\omega}_i \times l_{qi} \boldsymbol{\delta}_i = \mathbf{J}_{vqi} \mathbf{V}, \mathbf{J}_{vqi} = -l_{qi} \hat{\boldsymbol{\delta}}_i \mathbf{J}_{\omega i}
 \end{aligned}
 \tag{A12}$$

here, \mathbf{J}_{vgi} ($g = p, q$) is the translational Jacobian matrix of the moving link g_i in r_i .

In order to derive the formula for solving \mathbf{a}_{gi} , several items $\{r'_i, \boldsymbol{\delta}'_i, (\boldsymbol{\delta}'_i)^T, \boldsymbol{\delta}_i (\boldsymbol{\delta}'_i)^T, \boldsymbol{\delta}_i \boldsymbol{\delta}_i^T \hat{\boldsymbol{e}}_i', \hat{\boldsymbol{\delta}}_i \mathbf{J}'_{\omega i}, (i = 1, 2, 3)\}$ are derived as follows:

$$\begin{aligned}
 r'_i &= v_{ri} = \mathbf{r}'_i \cdot \boldsymbol{\delta}_i = (\mathbf{r}'_i)^T \boldsymbol{\delta}_i = (\mathbf{v} + \boldsymbol{\omega} \times \mathbf{e}_i)^T \boldsymbol{\delta}_i \\
 &= [(\mathbf{I} \quad -\hat{\boldsymbol{e}}_i) \mathbf{V}]^T \boldsymbol{\delta}_i = \mathbf{V}^T \begin{pmatrix} \mathbf{I} \\ \hat{\boldsymbol{e}}_i \end{pmatrix} \boldsymbol{\delta}_i = \mathbf{V}^T \begin{pmatrix} \boldsymbol{\delta}_i \\ \hat{\boldsymbol{e}}_i \boldsymbol{\delta}_i \end{pmatrix}, \\
 \boldsymbol{\delta}'_i &= (\mathbf{r}_i / r_i)' = -[(\mathbf{v} + \boldsymbol{\omega} \times \mathbf{e}_i) \times \boldsymbol{\delta}_i]^T \mathbf{C} \boldsymbol{\delta}_i / r_i \\
 &= -\left[\mathbf{V}^T \begin{pmatrix} \hat{\boldsymbol{\delta}}_i \\ \hat{\boldsymbol{e}}_i \hat{\boldsymbol{\delta}}_i \end{pmatrix} \right] \mathbf{C} \frac{\boldsymbol{\delta}_i}{r_i} = -\frac{\mathbf{V}^T}{r_i} \left[\begin{pmatrix} \hat{\boldsymbol{\delta}}_i \\ \hat{\boldsymbol{e}}_i \hat{\boldsymbol{\delta}}_i \end{pmatrix} \mathbf{C}_e \right] \boldsymbol{\delta}_i, \\
 \hat{\boldsymbol{\delta}}_i &= (\boldsymbol{\delta}'_i)^T \mathbf{C} = -\left(\mathbf{V}^T \begin{pmatrix} \hat{\boldsymbol{\delta}}_i^2 \\ \hat{\boldsymbol{e}}_i \hat{\boldsymbol{\delta}}_i^2 \end{pmatrix} \right) \frac{\mathbf{C}}{r_i} = -\mathbf{V}^T \left(\begin{pmatrix} \hat{\boldsymbol{\delta}}_i^2 \\ \hat{\boldsymbol{e}}_i \hat{\boldsymbol{\delta}}_i^2 \end{pmatrix} \frac{\mathbf{C}_e}{r_i} \right), \\
 \boldsymbol{\delta}_i \boldsymbol{\delta}_i^T \hat{\boldsymbol{e}}_i' &= -(\mathbf{e}_i')^T [(\boldsymbol{\delta}_i \boldsymbol{\delta}_i^T) \mathbf{C}] = -\mathbf{V}^T \begin{pmatrix} \mathbf{0} \\ \hat{\boldsymbol{e}}_i \end{pmatrix} [(\boldsymbol{\delta}_i \boldsymbol{\delta}_i^T) \mathbf{C}],
 \end{aligned}
 \tag{A13}$$

$$\begin{aligned}
 (\delta'_i)^T &= \{\delta_i \times [(\mathbf{v} + \boldsymbol{\omega} \times \mathbf{e}_i) \times \delta_i]\}^T / r_i \\
 &= - [(\mathbf{v} + \boldsymbol{\omega} \times \mathbf{e}_i) \times \delta_i]^T \frac{\hat{\delta}_i}{r_i} = - \frac{\mathbf{V}^T}{r_i} \begin{pmatrix} \hat{\delta}_i^2 \\ \hat{\mathbf{e}}_i \hat{\delta}_i^2 \end{pmatrix}, \\
 \delta_i (\delta'_i)^T &= \delta_i \{-s [(\mathbf{v} + \boldsymbol{\omega} \times \mathbf{e}_i) \times \delta_i] \delta_i / r_i\}^T \\
 &= - [(\mathbf{v} + \boldsymbol{\omega} \times \mathbf{e}_i) \times \delta_i]^T \frac{\delta_i \delta_i^T \mathbf{C}}{r_i} = - \mathbf{V}^T \begin{pmatrix} \hat{\delta}_i \\ \hat{\mathbf{e}}_i \hat{\delta}_i \end{pmatrix} \frac{(\delta_i \delta_i^T \mathbf{C})}{r_i}, \\
 \hat{\delta}_i \mathbf{J}'_{\omega i} &= \hat{\delta}_i [(J'_{\omega i1} \quad J'_{\omega i2}) - d'_{i1} \mathbf{J}_{\omega i}] / d_{i1} = \mathbf{V}^T \mathbf{h}, \\
 \hat{\delta}_i \mathbf{J}'_{\omega i1} &= \hat{\delta}_i (d'_{i2} \hat{\delta}_i^2)' = \hat{\delta}_i d'_{i2} \hat{\delta}_i^2 + \hat{\delta}_i d_{i2} (\hat{\delta}_i^2)' = \mathbf{V}^T \mathbf{h}_{i1}, \\
 \mathbf{h}_{i1} &= - \left(\mathbf{J}_{\omega i}^T \mathbf{R}_{i1} \mathbf{R}_{i2}^T - \begin{pmatrix} \mathbf{0} \\ \mathbf{I} \end{pmatrix} \mathbf{R}_{i2} \mathbf{R}_{i1}^T \right) (\hat{\delta}_i \mathbf{C}) \hat{\delta}_i^2 \\
 &\quad + \begin{pmatrix} \mathbf{I} \\ \hat{\mathbf{e}}_i \end{pmatrix} \frac{\hat{\delta}_i^2}{r_i} \left\{ (\hat{\delta}_i d_{i2} \mathbf{C}) \hat{\delta}_i + [(\hat{\delta}_i d_{i2}) \hat{\delta}_i] \mathbf{C} \right\}, \\
 \hat{\delta}_i \mathbf{J}'_{\omega i2} &= \hat{\delta}_i (d'_{i1} \mathbf{I} - d_{i2} \hat{\mathbf{r}}_i' - d_{i2} \hat{\mathbf{r}}_i - \mathbf{J}_{\omega i1} \hat{\mathbf{e}}_i' - \mathbf{J}_{\omega i1} \hat{\mathbf{e}}_i) = \mathbf{V}^T \mathbf{h}_{i2}, \\
 \mathbf{h}_{i2} &= \begin{pmatrix} \mathbf{I} \\ \hat{\mathbf{e}}_i \end{pmatrix} (\mathbf{R}_{i1} \times \mathbf{R}_{i2}) \hat{\delta}_i + \begin{pmatrix} \mathbf{0} \\ \mathbf{I} \end{pmatrix} \mathbf{R}_{i2} (r_i \cdot \mathbf{R}_{i1}) \hat{\delta}_i \\
 &\quad + \begin{pmatrix} \mathbf{I} \\ \hat{\mathbf{e}}_i \end{pmatrix} \left\{ [\hat{\delta}_i s (\mathbf{R}_{i2} \times \mathbf{R}_{i1})] \mathbf{C} \right\} + (\mathbf{J}_{\omega i}^T \mathbf{R}_{i1} \mathbf{R}_{i2}^T) (\hat{\delta}_i \mathbf{C}) \hat{\mathbf{r}}_i \\
 &\quad - \left(\begin{pmatrix} \mathbf{0} \\ \mathbf{I} \end{pmatrix} \mathbf{R}_{i2} \mathbf{R}_{i1}^T \right) (\hat{\delta}_i \mathbf{C}) \hat{\mathbf{r}}_i + \begin{pmatrix} \mathbf{0} \\ \hat{\mathbf{e}}_i \end{pmatrix} [(\hat{\delta}_i \mathbf{J}_{\omega i1}) \mathbf{C}] - \mathbf{h}_{i1} \hat{\mathbf{e}}_i, \\
 \mathbf{h} &= \frac{(\mathbf{h}_{i1} \quad \mathbf{h}_{i2})}{d_{i1}} - \left[\begin{pmatrix} \mathbf{I} \\ \hat{\mathbf{e}}_i \end{pmatrix} (\mathbf{R}_{i1} \times \mathbf{R}_{i2}) + \begin{pmatrix} \mathbf{0} \\ \mathbf{I} \end{pmatrix} \mathbf{R}_{i2} (r_i \cdot \mathbf{R}_{i1}) \right] \frac{\hat{\delta}_i \mathbf{J}_{\omega i}}{d_{i1}} \Big]
 \end{aligned}$$

Differentiating \mathbf{v}_{pi} ($i = 1, 2, 3$) in Eq. (A12), \mathbf{a}_{pi} is derived using Eqs. (A12) and (A13) as follows:

$$\begin{aligned}
 \mathbf{a}_{pi} &= \mathbf{v}'_{pi} = \mathbf{J}_{vpi} \mathbf{A} + \mathbf{J}'_{vpi} \mathbf{V}, \mathbf{J}'_{vpi} = \mathbf{V}^T \mathbf{H}_{vpi}, \\
 \mathbf{J}'_{vpi} &= \left[(\delta_i \delta_i^T \quad - (\delta_i \delta_i^T) \hat{\mathbf{e}}_i) - (r_i - l_{pi}) \hat{\delta}_i \mathbf{J}_{\omega i} \right]' \\
 &= \left[\left((\delta'_i \delta_i^T + \delta_i \delta_i'^T) \quad - (\delta'_i \delta_i^T + \delta_i \delta_i'^T) \hat{\mathbf{e}}_i - \delta_i \delta_i^T \hat{\mathbf{e}}_i' \right) \right. \\
 &\quad \left. - \left[(r_i - l_{pi})' \hat{\delta}_i + (r_i - l_{pi}) \hat{\delta}_i' \right] \mathbf{J}_{\omega i} - (r_i - l_{pi}) \hat{\delta}_i \mathbf{J}'_{\omega i}, \right. \tag{A14} \\
 \mathbf{H}_{vpi} &= (\mathbf{h}_{pi1} \quad \mathbf{h}_{pi2}) - (r_i - l_{pi}) \mathbf{h} \\
 &\quad - \begin{pmatrix} \mathbf{I} \\ \hat{\mathbf{e}}_i \end{pmatrix} \left[\delta_i \hat{\delta}_i - (r_i - l_{pi}) \frac{\hat{\delta}_i^2}{r_i} \mathbf{C}_e \right] \mathbf{J}_{\omega i}, \\
 \mathbf{h}_{pi1} &= - \frac{1}{r_i} \left\{ \left(\begin{pmatrix} \hat{\delta}_i \\ \hat{\mathbf{e}}_i \hat{\delta}_i \end{pmatrix} \mathbf{C}_e \right) \delta_i \delta_i^T + \begin{pmatrix} \hat{\delta}_i \\ \hat{\mathbf{e}}_i \hat{\delta}_i \end{pmatrix} [(\delta_i \delta_i^T) \mathbf{C}] \right\}, \\
 \mathbf{h}_{pi2} &= - \mathbf{h}_{pi1} \hat{\mathbf{e}}_i + \begin{pmatrix} \mathbf{0} \\ \hat{\mathbf{e}}_i \end{pmatrix} [(\delta_i \delta_i^T) \mathbf{C}]
 \end{aligned}$$

Differentiating \mathbf{v}_{qi} ($i = 1, 2, 3$) in Eq. (A12), \mathbf{a}_{qi} is derived using Eqs. (A12) as follows:

$$\mathbf{a}_{qi} = \mathbf{J}_{vqi}\mathbf{A} + \mathbf{J}'_{vqi}\mathbf{V}, \mathbf{J}'_{vqi} = \left(-l_{qi}\hat{\delta}_i\mathbf{J}_{\omega i}\right)' = -l_{qi}\left(\hat{\delta}'_i\mathbf{J}_{\omega i} + \hat{\delta}_i\mathbf{J}'_{\omega i}\right) = \mathbf{V}^T\mathbf{H}_{vqi},$$

$$\mathbf{H}_{vqi} = \frac{l_{qi}}{r_i}\left(\frac{\hat{\delta}_i^2}{\hat{\mathbf{e}}_i\hat{\delta}_i}\right)\mathbf{C}_e\mathbf{J}_{\omega i} - l_{qi}\mathbf{h}$$
(A15)

A.3. Velocity and acceleration of moving links in r_0

Let $\boldsymbol{\omega}_0$ and $\boldsymbol{\varepsilon}_0$ be the angular velocity and the angular acceleration of r_0 in $\{B\}$, respectively. Since the upper end of r_0 is fixed onto m at o and $r_0|z$ is satisfied, $\boldsymbol{\omega}_0 = \boldsymbol{\omega}$ and $\boldsymbol{\varepsilon}_0 = \boldsymbol{\varepsilon}$ are satisfied. r_0 is composed of a piston rod with its mass center p_0 and a cylinder with its mass center q_0 . Let r_0 be the distance from O to o . Let l_{p0} be the distance from o to p_0 . Let l_{q0} be the distance from O to q_0 . Let \mathbf{v}_{g0} and \mathbf{a}_{g0} be respectively the translational velocity and the acceleration of the moving link g_0 in r_0 at its mass center in $\{B\}$, $g = p$ for the piston rod, $g = q$ for the cylinder. As $i = 0$, $e_i = 0$ are satisfied, the angular velocity and translational velocity kinematics of g_0 are represented as follows:

$$\boldsymbol{\omega}_0 = \mathbf{J}_{\omega 0}\mathbf{V} = \boldsymbol{\omega}, \mathbf{J}_{\omega 0} = \begin{pmatrix} \mathbf{0} & \mathbf{I} \end{pmatrix}, \mathbf{J}'_{\omega 0} = \mathbf{V}^T\mathbf{H}_{\omega 0},$$

$$\boldsymbol{\varepsilon}_0 = \mathbf{J}_{\omega 0}\mathbf{A} + \mathbf{V}^T\mathbf{H}_{\omega 0}\mathbf{V} = \mathbf{J}_{\omega 0}\mathbf{A} = \boldsymbol{\varepsilon},$$

$$\mathbf{H}_{\omega 0} = \mathbf{0}, \mathbf{J}'_{\omega 0} = \mathbf{0}, \mathbf{v}_{p0} = \mathbf{J}_{vp0}\mathbf{V}, \mathbf{v}_{q0} = \mathbf{J}_{vq0}\mathbf{V},$$

$$\mathbf{J}_{vp0} = \delta_0\delta_0^T(\mathbf{I} \ \mathbf{0}) - (r_0 - l_{p0})\hat{\delta}_0\mathbf{J}_{\omega 0}, \mathbf{J}_{vq0} = -l_{q0}\hat{\delta}_0\mathbf{J}_{\omega 0}$$
(A16)

here, $\mathbf{J}_{\omega 0}$ is the 3×6 rotational Jacobian matrix of r_0 ; $\mathbf{H}_{\omega 0}$ is the 3×6 rotational Hessian matrix of r_0 .

The several items $\{\delta'_0, (\delta'_0)^T, \delta_0(\delta'_0)^T\}$ for solving \mathbf{a}_{g0} are derived from Eqs. (A13) as follows:

$$\delta'_0 = -\frac{\mathbf{V}^T}{r_0}\begin{pmatrix} \hat{\delta}_0 \\ \mathbf{0} \end{pmatrix}\mathbf{C}_e\delta_0, (\delta'_0)^T = -\frac{\mathbf{V}^T}{r_0}\begin{pmatrix} \hat{\delta}_0^2 \\ \mathbf{0} \end{pmatrix},$$

$$\delta_0\delta_0^T = -\frac{\mathbf{V}^T}{r_0}\begin{pmatrix} \hat{\delta}_0 \\ \mathbf{0} \end{pmatrix}(\delta_0\delta_0^T\mathbf{C})$$
(A17)

Differentiating \mathbf{v}_{p0} in Eq. (A16), the formulas for solving \mathbf{a}_{p0} are derived using Eqs. (A16) and (A17) as follows:

$$\mathbf{a}_{p0} = \mathbf{J}_{vp0}\mathbf{A} + \mathbf{J}'_{vp0}\mathbf{V} = \mathbf{J}_{vp0}\mathbf{A} + \mathbf{V}^T\mathbf{H}_{vp0}\mathbf{V},$$

$$\mathbf{J}'_{vp0} = \left[\delta_0\delta_0^T(\mathbf{I} \ \mathbf{0}) - (r_0 - l_{p0})\hat{\delta}_0\mathbf{J}_{\omega 0}\right]' = \mathbf{V}^T\mathbf{H}_{vp0},$$

$$\mathbf{H}_{vp0} = \left(-\left(\begin{pmatrix} \hat{\delta}_0 \\ \mathbf{0} \end{pmatrix}\mathbf{C}_e\right)\frac{\delta_0\delta_0^T}{r_0} - \frac{1}{r_0}\begin{pmatrix} \hat{\delta}_0 \\ \mathbf{0} \end{pmatrix}\left[(\delta_0\delta_0^T)\mathbf{C}\right] \ \mathbf{0}\right)$$

$$-\begin{pmatrix} \hat{\delta}_0 \\ \mathbf{0} \end{pmatrix}\hat{\delta}_0\mathbf{J}_{\omega 0} + \frac{(r_0 - l_{p0})}{r_0}\begin{pmatrix} \hat{\delta}_0^2 \\ \mathbf{0} \end{pmatrix}\mathbf{C}_e\mathbf{J}_{\omega 0}$$
(A18)

here, \mathbf{H}_{vp0} is the 6×6 translational Hessian matrix of the piston rod as $g = p$ in r_0 .

Differentiating \mathbf{v}_{q0} in Eq. (A16), the formulas for solving \mathbf{a}_{q0} are derived using Eqs. (A16) and (A17) as follows:

$$\mathbf{a}_{q0} = \mathbf{J}_{vq0}\mathbf{A} + \mathbf{V}^T\mathbf{H}_{vq0}\mathbf{V}, \mathbf{H}_{vq0} = \frac{l_{q0}}{r_0}\begin{pmatrix} \hat{\delta}_0^2 \\ \mathbf{0} \end{pmatrix}\mathbf{C}_e\mathbf{J}_{\omega 0},$$

$$\mathbf{J}'_{vq0} = \left(-l_{q0}\hat{\delta}_0\mathbf{J}_{\omega 0}\right)' = -l_{q0}\left[(\delta'_0)^T\mathbf{C}\right]\mathbf{J}_{\omega 0} = \mathbf{V}^T\mathbf{H}_{vq0}$$
(A19)

here, \mathbf{H}_{vq0} is the 6×6 translational Hessian matrix of the cylinder rod in r_0 .

The formulas for solving the general velocity V_{g_i} and the general acceleration A_{g_i} of the moving links g_i in r_i ($i = 0, 1, 2, 3$) are represented as follows:

$$V_{g_i} = \begin{pmatrix} v_{g_i} \\ \omega_i \end{pmatrix} = J_{g_i} V, \quad J_{g_i} = \begin{pmatrix} J_{v_{g_i}} \\ J_{\omega_i} \end{pmatrix}, \quad J'_{g_i} = V^T H_{g_i}, \tag{A20}$$

$$A_{g_i} = \begin{pmatrix} a_{g_i} \\ \epsilon_i \end{pmatrix} = J_{g_i} A + V^T H_{g_i} V, \quad H_{g_i} = \begin{pmatrix} H_{v_{g_i}} \\ H_{\omega_i} \end{pmatrix}, \quad i = 0, 1, 2, 3; \quad g = p, q$$

Appendix B

A logical block of equivalent simulation mechanism of the gripper with three fingers and its simulation mechanism are constructed by Matlab/Simulink/Mechanics, see Fig. B1.

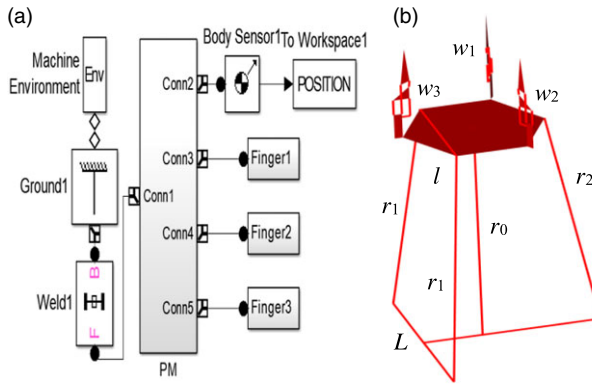


Figure B1. A logical block of equivalent simulation mechanism of the gripper with three fingers (a) and its simulation mechanism (b)

A logical block of parallel wrist is constructed using Matlab/Simulink/Mechanics, see Fig. B2.

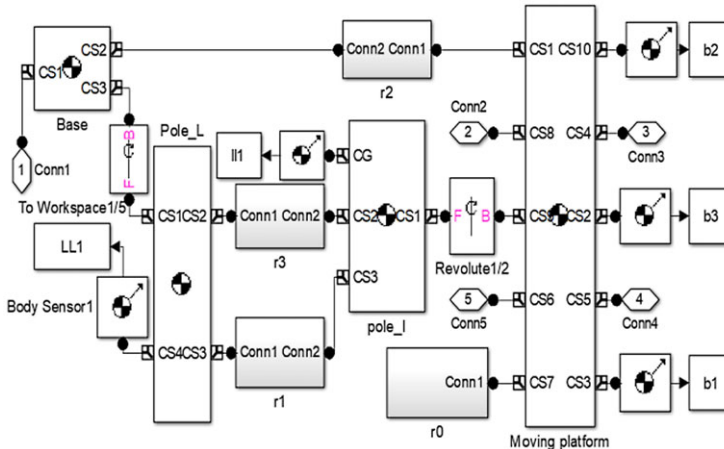


Figure B2. A logical block of parallel wrist

A logical block of RPR-type actuation limbs r_1, r_3 are constructed using Matlab/Simulink/Mechanics, see Fig. B3.

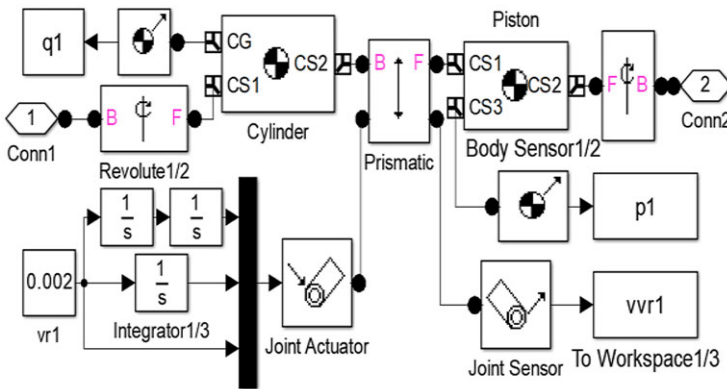


Figure B3. Logical block of RPR-type actuation limb r_1 .

A logical block of finger is constructed using Matlab/Simulink/Mechanics [20], see Fig. B4.

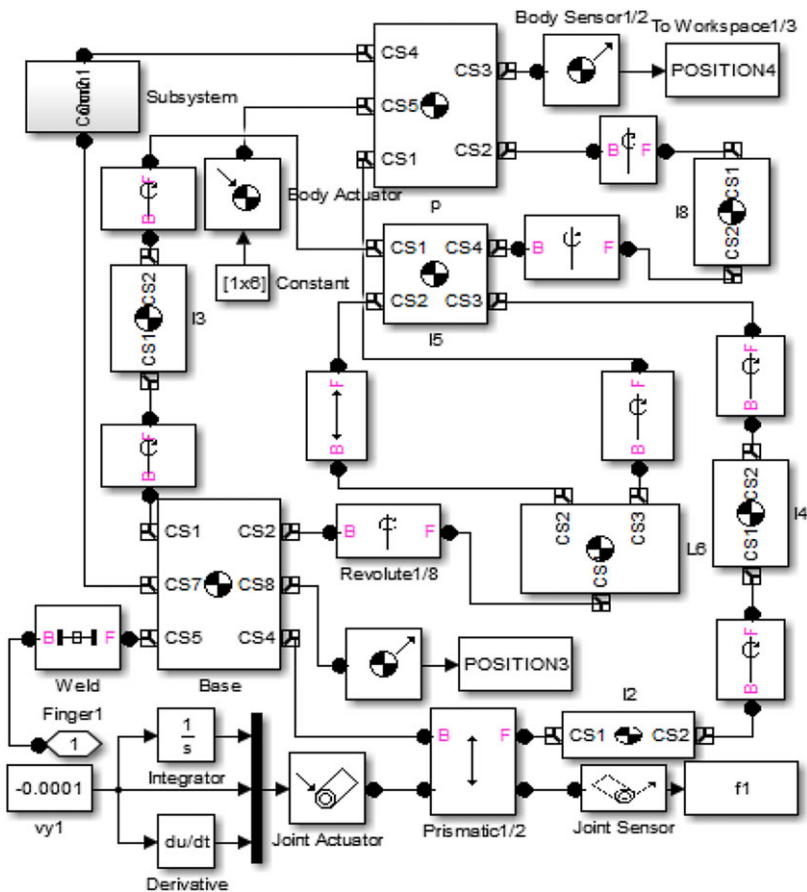


Figure B4. A logical block of finger.

Table B1. Absolute errors $\Delta x = \text{abs}(x - x_s)$ between the maximum theoretical solutions x and the maximum simulation solutions x_s

| | | | | | | | | |
|----------------------------|----------------------------|----------------------------|----------------------------|----------------------------|----------------------------|----------------------------|----------------------------|----------------------------|
| Δv_{q0x} | Δv_{q0y} | Δv_{q0z} | Δa_{q0x} | Δa_{q0y} | Δa_{q0z} | $\Delta \omega_{r0x}$ | $\Delta \omega_{r0y}$ | $\Delta \omega_{r0z}$ |
| 1.02 $\times 10^{-14}$ | 3.73 $\times 10^{-14}$ | 9.99 $\times 10^{-15}$ | 6.35 $\times 10^{-12}$ | 3.79 $\times 10^{-12}$ | 1.30 $\times 10^{-12}$ | -3.85 $\times 10^{-13}$ | 9.95 $\times 10^{-14}$ | 1.07 $\times 10^{-14}$ |
| Δv_{p0x} | Δv_{p0y} | Δv_{p0z} | Δa_{p0x} | Δa_{p0y} | Δa_{p0z} | $\Delta \varepsilon_{r0x}$ | $\Delta \varepsilon_{r0y}$ | $\Delta \varepsilon_{r0z}$ |
| -1.07 $\times 10^{-14}$ | 7.58 $\times 10^{-14}$ | -1.01 $\times 10^{-13}$ | 6.25 $\times 10^{-12}$ | 3.73 $\times 10^{-12}$ | 1.69 $\times 10^{-12}$ | $\leq 10^{-16}$ | $\leq 10^{-16}$ | $\leq 10^{-16}$ |
| Δv_{q1x} | Δv_{q1y} | Δv_{q1z} | Δa_{q1x} | Δa_{q1y} | Δa_{q1z} | $\Delta \omega_{r1x}$ | $\Delta \omega_{r1y}$ | $\Delta \omega_{r1z}$ |
| 1.02 $\times 10^{-14}$ | 3.74 $\times 10^{-14}$ | 9.99 $\times 10^{-15}$ | 9.99 $\times 10^{-16}$ | 9.99 $\times 10^{-16}$ | 1.11 $\times 10^{-16}$ | -3.81 $\times 10^{-13}$ | 1.03 $\times 10^{-13}$ | 1.07 $\times 10^{-14}$ |
| Δv_{p1x} | Δv_{p1y} | Δv_{p1z} | Δa_{p1x} | Δa_{p1y} | Δa_{p1z} | $\Delta \varepsilon_{r1x}$ | $\Delta \varepsilon_{r1y}$ | $\Delta \varepsilon_{r1z}$ |
| -9.95 $\times 10^{-14}$ | 7.69 $\times 10^{-14}$ | -1.07 $\times 10^{-14}$ | 9.99 $\times 10^{-15}$ | 9.99 $\times 10^{-15}$ | 9.99 $\times 10^{-15}$ | 9.99 $\times 10^{-15}$ | 9.77 $\times 10^{-15}$ | 9.99 $\times 10^{-16}$ |
| Δv_{q2x} | Δv_{q2y} | Δv_{q2z} | Δa_{q2x} | Δa_{q2y} | Δa_{q2z} | $\Delta \omega_{r2x}$ | $\Delta \omega_{r2y}$ | $\Delta \omega_{r2z}$ |
| 1.02 $\times 10^{-14}$ | 2.42 $\times 10^{-13}$ | -3.72 $\times 10^{-14}$ | -4.95 $\times 10^{-12}$ | -1.22 $\times 10^{-12}$ | -3.96 $\times 10^{-12}$ | 6.33 $\times 10^{-13}$ | -1.07 $\times 10^{-13}$ | 1.07 $\times 10^{-14}$ |
| Δv_{p2x} | Δv_{p2y} | Δv_{p2z} | Δa_{p2x} | Δa_{p2y} | Δa_{p2z} | $\Delta \varepsilon_{r2x}$ | $\Delta \varepsilon_{r2y}$ | $\Delta \varepsilon_{r2z}$ |
| 1.07 $\times 10^{-14}$ | 9.45 $\times 10^{-14}$ | 1.82 $\times 10^{-14}$ | -2.16 $\times 10^{-12}$ | 4.43 $\times 10^{-13}$ | 5.01 $\times 10^{-13}$ | 4.51 $\times 10^{-12}$ | 2.23 $\times 10^{-11}$ | -2.96 $\times 10^{-12}$ |
| Δv_{q3x} | Δv_{q3y} | Δv_{q3z} | Δa_{q3x} | Δa_{q3y} | Δa_{q3z} | $\Delta \omega_{r3x}$ | $\Delta \omega_{r3y}$ | $\Delta \omega_{r3z}$ |
| -1.02 $\times 10^{-14}$ | 3.73 $\times 10^{-14}$ | -6.00 $\times 10^{-15}$ | -4.83 $\times 10^{-12}$ | -7.42 $\times 10^{-12}$ | -3.93 $\times 10^{-12}$ | -3.81 $\times 10^{-13}$ | 1.07 $\times 10^{-13}$ | -2.04 $\times 10^{-14}$ |
| Δv_{p3x} | Δv_{p3y} | Δv_{p3z} | Δa_{p3x} | Δa_{p3y} | Δa_{p3z} | $\Delta \varepsilon_{r3x}$ | $\Delta \varepsilon_{r3y}$ | $\Delta \varepsilon_{r3z}$ |
| -2.04 $\times 10^{-14}$ | -7.68 $\times 10^{-14}$ | 1.07 $\times 10^{-14}$ | -1.97 $\times 10^{-12}$ | 3.00 $\times 10^{-14}$ | -1.80 $\times 10^{-13}$ | -1.02 $\times 10^{-14}$ | 1.93 $\times 10^{-11}$ | -3.96 $\times 10^{-12}$ |
| $\Delta \omega_L$ | $\Delta \varepsilon_L$ | Δf_{a1} | Δf_{a2} | Δf_{a3} | Δf_{c01} | Δf_{c02} | Δf_c | |
| -1.01 $\times 10^{-13}$ | -1.02 $\times 10^{-14}$ | -2.47 $\times 10^{-7}$ | 4.49 $\times 10^{-7}$ | -2.31 $\times 10^{-7}$ | -4.12 $\times 10^{-5}$ | 1.36 $\times 10^{-6}$ | 9.50 $\times 10^{-8}$ | |

Cite this article: Y. Lu, Z. Chang and Y. Lu (2023). "Development and dynamics of a novel couple-constrained parallel wrist with three measuring force flexible fingers", *Robotica* **41**, 2713–2734. <https://doi.org/10.1017/S0263574723000620>